Table 2. The establishment efficiency of EBV latency

Cell	Emergence of G418-resistant cells†	
BJAB	100%	(6/6)
Daudi	100%	(10/10)
BALL-1		
Parental	56%	(5/9)
GFP Hi	67%	(2/3)
GFP-dnE1 Hi	0%	(0/6)
GFP-dnE1 Lo	0%	(0/6)

†Percentage of wells positive for G418-resistant cells over the number of tested wells from 96-well plates indicated in the bracket. Shown are the sum of two independent experiments. dnE1, dominant-negative EBNA1; EBV, Epstein–Barr virus; GFP, green fluorescent protein.

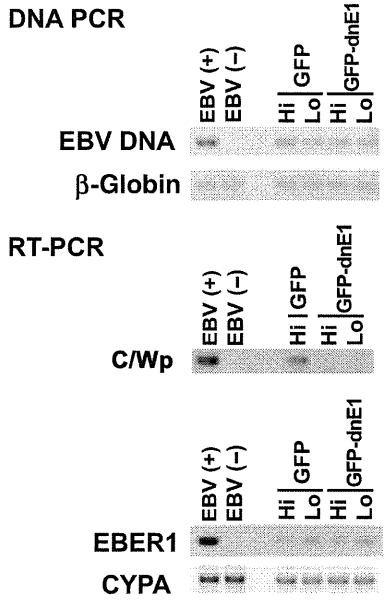

Fig. 4. PCR-based analysis of Epstein–Barr virus (EBV) gene expression. The effect of green fluorescent protein (GFP)-dominant-negative EBNA1 (dnE1) on the loss of EBV DNA (DNA PCR, upper panels) and transcription of the C/W promoter-driven transcript (C/Wp), EBER1, and cyclophilin A (CYPA; RT-PCR, lower panels) in BALL-1 cells at 2 days post-infection were examined. EBV-transformed B-lymphoblastoid cell line (B-LCL) and BJAB cells, denoted as EBV(+) and EBV(−), were used as positive and negative controls for viral DNA and RNA shown, respectively. β-Globin and CYPA were used as controls.

Table 3. Quantification of EBV transcripts in BALL-1 cells by real-time PCR at 2 days post-infection

BALL-1 cells		W1/2 exon (copies†)	EBER1 (copies‡)	CYPA (copies‡)
GFP	Hi	2.2	2.8×10^2	1.4×10^6
	Lo	NT§	0.8×10^2	1.0×10^6
GFP-dnE1	Hi	BLD¶	3.3×10^2	1.3×10^6
	Lo	BLD¶	1.2×10^2	1.5×10^6

†Copies per 13–14 ng total cellular RNA. ‡Copies per 200 ng total cellular RNA. §Not tested. ¶Below the limit of detection. CYPA, cyclophilin A; dnE1, dominant-negative EBNA1; EBV, Epstein–Barr virus; GFP, green fluorescent protein.

tion from C/Wp. Taken together, these results show that inhibition of EBNA1 functions strongly restricts EBV-encoded transforming gene expression and, although there is no detectable effect on the ROL of EBV DNA at the acute phase of viral infection, it blocks the establishment of EBV latency during the subacute phase.

Discussion

This is the first report describing the effect of EBNA1 inhibition from the onset of EBV infection in B cells. Unexpectedly, the dnE1 was unable to accelerate the ROL during the acute phase of EBV infection since dnE1 enhanced the loss of the oriP plasmid in the transient transfection assays.[10,11] In the subacute phase of EBV infection, the establishment of EBV latency was potently blocked by dnE1. In addition, we observed a strong repressive effect of dnE1 on the EBNA1-dependent enhancement of viral gene transcription from C/Wp during the early phase of EBV infection, similar to the transient transfection assays.[17] These data suggest that viral oncogene expression depends heavily on EBNA1 during the acute phase of viral infection, and that EBNA1 contributes little to EBV genome maintenance during this period. The results emphasize that an EBNA1 inhibitor should serve as an attenuator of viral oncogene expression since activation of C/Wp is the 'root' event of the positive feedback loop involved in the transactivation of viral transforming gene expression. In this regard, the EBNA1 inhibition approach could be superior to LMP-1 or EBNA2 inhibition.

If EBNA1 binding to oriP is essential for both the enhancement of viral gene transcription and for genome maintenance, what mechanism prevents dnE1 from affecting the ROL during the acute phase of EBV infection? It is likely that maintenance of the oriP replicon immediately after its introduction into cells is less efficient than in cells harboring an 'established' oriP replicon as an autonomously replicating plasmid. The ROL of an established oriP replicon is 2–4% per cell generation.[10,11] In contrast, our data from the EBV/B cell-based assay gave an average ROL of 26–38% during the week post-infection (acute phase of EBV infection). In agreement with our findings, it is reported that a transiently transduced oriP replicon is lost from cells at 26–37% per cell generation 1–2 weeks post-plasmid transduction.[12] These data indicate that maintenance of the oriP replicon is largely EBNA1-independent immediately after its introduction into cells, regardless of whether the route of introduction is by transfection or EBV infection. In other words, the establishment of EBV latency should be a rare epigenetic event. The data also suggest that the artificial minichromosome approach may be relevant in understanding EBV genome behavior.[12]

Our study suggests that gene therapy using GFP-dnE1 is an attractive approach, not only for therapeutics, but also for prophylactic interventions of EBV-associated malignancies. For example, in peripheral blood stem cell transplantation (PBSCT), GFP-dnE1 transduction into $CD34^+$ cells should protect the differentiated B cells from EBV infection, thus preventing the genesis of EBV-associated B cell lymphomas. We will attempt to prove this hypothesis using a small animal model in future studies.[26] Additionally, EBNA1 is a potential molecular target for developing a small molecular-weight EBV inhibitor as mentioned previously.[14,15] The advantages of EBNA1-inhibitor development are that the biological assay system is already established and the X-ray crystal structure of the DNA-bound EBNA1 DNA binding and dimerization domain is known, which means that computer-aided drug design technology can be immediately applied. Although EBV is associated with various malignancies, preventive and therapeutic measures against EBV infection have not been developed. We believe that an anti-EBV agent, such as an EBNA1 inhibitor, would have an enormous impact in the medical field due to the substantial number of patients with EBV-associated malignancies.

doi: 10.1111/j.1349-7006.2009.01474.x

Acknowledgments

We thank Drs Kenichi Imadome and Shigeyoshi Fujiwara for reagents. We also thank Dr Bill Sugden for critically reading the manuscript. This work was supported by the Japan Health Science Foundation, the Ministry of Health, Labor and Welfare of Japan, and the Ministry of Education, Culture, Sports, Science and Technology of Japan.

Disclosure Statement

The authors have no conflict of interest.

References

1 Thompson MP, Kurzrock R. Epstein–Barr virus and cancer. *Clin Cancer Res* 2004; **10**: 803–21.
2 Rickinson AB, Kieff E. Epstin–Barr virus. In: Knipe DM, Howley PM, eds. *Fields Virology*, 5th edn, vol. 2. Philadelphia: Lippincott Williams & Wilkins, 2007; 2655–700.
3 Klein E, Kis LL, Klein G. Epstein–Barr virus infection in humans: from harmless to life endangering virus-lymphocyte interactions. *Oncogene* 2007; **26**: 1297–305.
4 Snow AL, Martinez OM. Epstein–Barr virus: evasive maneuvers in the development of PTLD. *Am J Transplant* 2007; **7**: 271–7.
5 Besson C, Goubar A, Gabarre J *et al.* Changes in AIDS-related lymphoma since the era of highly active antiretroviral therapy. *Blood* 2001; **98**: 2339–44.
6 Carbone A, Cesarman E, Spina M, Gloghini A, Schulz TF. HIV-associated lymphomas and gamma-herpesviruses. *Blood* 2009; **113**: 1213–24.
7 Kieff E, Rickinson AB. Epstin–Barr virus and its replication. In: Knipe DM, Howley PM, eds. *Fields Virology*, 5th edn, vol. 2. Philadelphia: Lippincott Williams & Wilkins, 2007; 2603–54.
8 Lindner SE, Sugden B. The plasmid replicon of Epstein–Barr virus: mechanistic insights into efficient, licensed, extrachromosomal replication in human cells. *Plasmid* 2007; **58**: 1–12.
9 Wang J, Sugden B. Origins of bidirectional replication of Epstein–Barr virus: models for understanding mammalian origins of DNA synthesis. *J Cell Biochem* 2005; **94**: 247–56.
10 Kirchmaier AL, Sugden B. Plasmid maintenance of derivatives of oriP of Epstein–Barr virus. *J Virol* 1995; **69**: 1280–3.
11 Sugden B, Warren N. Plasmid origin of replication of Epstein–Barr virus, oriP, does not limit replication in cis. *Mol Biol Med* 1988; **5**: 85–94.
12 Leight ER, Sugden B. Establishment of an oriP replicon is dependent upon an infrequent, epigenetic event. *Mol Cell Biol* 2001; **21**: 4149–61.
13 Hurley EA, Thorley-Lawson DA. B cell activation and the establishment of Epstein–Barr virus latency. *J Exp Med* 1988; **168**: 2059–75.
14 Altmann M, Pich D, Ruiss R, Wang J, Sugden B, Hammerschmidt W. Transcriptional activation by EBV nuclear antigen 1 is essential for the expression of EBV's transforming genes. *Proc Natl Acad Sci U S A* 2006; **103**: 14188–93.
15 Kennedy G, Komano J, Sugden B. Epstein–Barr virus provides a survival factor to Burkitt's lymphomas. *Proc Natl Acad Sci U S A* 2003; **100**: 14269–74.
16 Nasimuzzaman M, Kuroda M, Dohno S *et al.* Eradication of Epstein–Barr virus episome and associated inhibition of infected tumor cell growth by adenovirus vector-mediated transduction of dominant-negative EBNA1. *Mol Ther* 2005; **11**: 578–90.
17 Kirchmaier AL, Sugden B. Dominant-negative inhibitors of EBNA-1 of Epstein–Barr virus. *J Virol* 1997; **71**: 1766–75.
18 Komano J, Miyauchi K, Matsuda Z, Yamamoto N. Inhibiting the Arp2/3 complex limits infection of both intracellular mature vaccinia virus and primate lentiviruses. *Mol Biol Cell* 2004; **15**: 5197–207.
19 Aiyar A, Sugden B. Fusions between Epstein–Barr viral nuclear antigen-1 of Epstein–Barr virus and the large T-antigen of simian virus 40 replicate their cognate origins. *J Biol Chem* 1998; **273**: 33073–81.
20 Middleton T, Sugden B. EBNA1 can link the enhancer element to the initiator element of the Epstein–Barr virus plasmid origin of DNA replication. *J Virol* 1992; **66**: 489–95.
21 Urano E, Kariya Y, Futahashi Y *et al.* Identification of the P-TEFb complex-interacting domain of Brd4 as an inhibitor of HIV-1 replication by functional cDNA library screening in MT-4 cells. *FEBS Lett* 2008; **582**: 4053–8.
22 Shimizu S, Urano E, Futahashi Y *et al.* Inhibiting lentiviral replication by HEXIM1, a cellular negative regulator of the CDK9/cyclin T complex. *AIDS* 2007; **21**: 575–82.
23 Kanda T, Yajima M, Ahsan N, Tanaka M, Takada K. Production of high-titer Epstein–Barr virus recombinants derived from Akata cells by using a bacterial artificial chromosome system. *J Virol* 2004; **78**: 7004–15.
24 Mackey D, Sugden B. The linking regions of EBNA1 are essential for its support of replication and transcription. *Mol Cell Biol* 1999; **19**: 3349–59.
25 Howe JG, Shu MD. Epstein–Barr virus small RNA (EBER) genes: unique transcription units that combine RNA polymerase II and III promoter elements. *Cell* 1989; **57**: 825–34.
26 Yajima M, Imadome K, Nakagawa A *et al.* A new humanized mouse model of Epstein–Barr virus infection that reproduces persistent infection, lymphoproliferative disorder, and cell-mediated and humoral immune responses. *J Infect Dis* 2008; **198**: 673–82.

Journal of General Virology (2010), **91**, 42–50 DOI 10.1099/vir.0.013482-0

Quantitative analysis of Epstein–Barr virus (EBV)-related gene expression in patients with chronic active EBV infection

Seiko Iwata,[1] Kaoru Wada,[1] Satomi Tobita,[1] Kensei Gotoh,[2] Yoshinori Ito,[2] Ayako Demachi-Okamura,[3] Norio Shimizu,[4] Yukihiro Nishiyama[1] and Hiroshi Kimura[1]

Correspondence
Hiroshi Kimura
hkimura@med.nagoya-u.ac.jp

[1]Department of Virology, Nagoya University Graduate School of Medicine, Nagoya, Japan

[2]Department of Pediatrics, Nagoya University Graduate School of Medicine, Nagoya, Japan

[3]Division of Immunology, Aichi Cancer Center Research Institute, Nagoya, Japan

[4]Department of Virology, Division of Medical Science, Medical Research Institute, Graduate School of Medicine, Tokyo Medical and Dental University, Tokyo, Japan

Chronic active Epstein–Barr virus (CAEBV) infection is a systemic Epstein–Barr virus (EBV)-positive lymphoproliferative disorder characterized by persistent or recurrent infectious mononucleosis-like symptoms in patients with no known immunodeficiency. The detailed pathogenesis of the disease is unknown and no standard treatment regimen has been developed. EBV gene expression was analysed in peripheral blood samples collected from 24 patients with CAEBV infection. The expression levels of six latent and two lytic EBV genes were quantified by real-time RT-PCR. EBV-encoded small RNA 1 and *Bam*HI-A rightward transcripts were abundantly detected in all patients, and latent membrane protein (LMP) 2 was observed in most patients. EBV nuclear antigen (EBNA) 1 and LMP1 were detected less frequently and were expressed at lower levels. EBNA2 and the two lytic genes were not detected in any of the patients. The pattern of latent gene expression was determined to be latency type II. EBNA1 was detected more frequently and at higher levels in the clinically active patients. Quantifying EBV gene expression is useful in clarifying the pathogenesis of CAEBV infection and may provide information regarding a patient's disease prognosis, as well as possible therapeutic interventions.

Received 22 May 2009
Accepted 25 September 2009

INTRODUCTION

Epstein–Barr virus (EBV) is the causative agent of infectious mononucleosis and is associated with several malignancies, including Burkitt's lymphoma, Hodgkin's lymphoma, nasopharyngeal carcinoma and post-transplant lymphoproliferative disorders (Cohen, 2000; Rickinson & Kieff, 2007; Williams & Crawford, 2006). Chronic active EBV (CAEBV) infection is a systemic EBV-positive lymphoproliferative disorder characterized by persistent or recurrent infectious mononucleosis-like symptoms in patients with no known immunodeficiency (Kimura, 2006; Okano *et al.*, 2005; Straus, 1988; Tosato *et al.*, 1985). The clonal expansion of EBV-infected T cells or natural killer (NK) cells plays a pathogenic role in patients with CAEBV, particularly among those in east Asia or central America (Kanegane *et al.*, 2002; Kimura, 2006; Quintanilla-Martinez *et al.*, 2000). These patients can be classified into two groups based on the predominantly infected cell type, T cells or NK cells (Kimura *et al.*, 2001, 2003). Nonetheless, the detailed pathogenesis of CAEBV remains elusive and no standard treatment regimen has been developed. Recently, haematopoietic stem cell transplantation (HSCT) was introduced as a curative therapy for CAEBV (Fujii *et al.*, 2000; Okamura *et al.*, 2000; Taketani *et al.*, 2002); however, transplant-related complications are common in such patients (Gotoh *et al.*, 2008; Kimura *et al.*, 2001, 2003). Alternatively, the EBV-related antigens expressed by infected cells are possible targets for treatment with EBV-specific cytotoxic T lymphocytes (CTLs) (Heslop *et al.*, 1996; Rooney *et al.*, 1998).

Viral gene expression in EBV-associated diseases is classified into one of three latency patterns (Cohen, 2000; Kieff & Rickinson, 2007). Latency type I, which is found in Burkitt's lymphoma, is characterized by EBV nuclear antigen (EBNA) 1, EBV-encoded small RNAs (EBERs) and *Bam*HI-A rightward transcripts (BARTs) expression (Tao *et al.*, 1998). In latency type II, which is characteristic

A supplementary table of primer sequences is available with the online version of this paper.

of Hodgkin's lymphoma and nasopharyngeal carcinoma, EBNA1, latent membrane protein (LMP) 1, LMP2, EBERs and BARTs are expressed (Brooks *et al.*, 1992; Deacon *et al.*, 1993). In latency type III, which is associated with post-transplant lymphoproliferative disorders, all of the above latent genes (EBNA1, EBNA2, EBNA3A, 3B, 3C, EBNA-LP, LMP1, LMP2, EBERs and BARTs) are expressed (Young *et al.*, 1989).

We recently reported that EBV gene expression could be quantitatively assessed by multiplex real-time RT-PCR (Kubota *et al.*, 2008). This method not only helps quantify EBV gene expression but also can be used to clarify the pathogenesis of EBV-associated diseases and to provide information about their prognosis and possible therapeutic interventions. Thus, in this study, we quantified the expression of six latent (EBNA1, EBNA2, LMP1, LMP2, EBER1 and BARTs) and two lytic [BZLF1 and glycoprotein (gp) 350/220] EBV genes in the peripheral blood of patients with CAEBV.

RESULTS

First, we quantified the expression of several EBV genes in B, T and NK cell lines by real-time RT-PCR (Fig. 1a). In the EBV-positive B cell lines (Raji, LCL-1 and LCL-2), all six latent genes (EBNA1, EBNA2, LMP1, LMP2, EBER1 and BARTs) were detected, and the gene expression pattern was consistent with latency type III. Both lytic genes were detected in LCL-1 and -2 cells. However, none of the target genes was detected in BJAB, an EBV-negative cell line. EBNA1, LMP1, LMP2, EBER1 and BARTs, but not EBNA2, were detected in both the T (SNT-8, -13, -15 and -16) and NK cell lines (SNK-1, -6, -10 and KAI-3). The pattern of expression in the T and NK cell lines was latency type II.

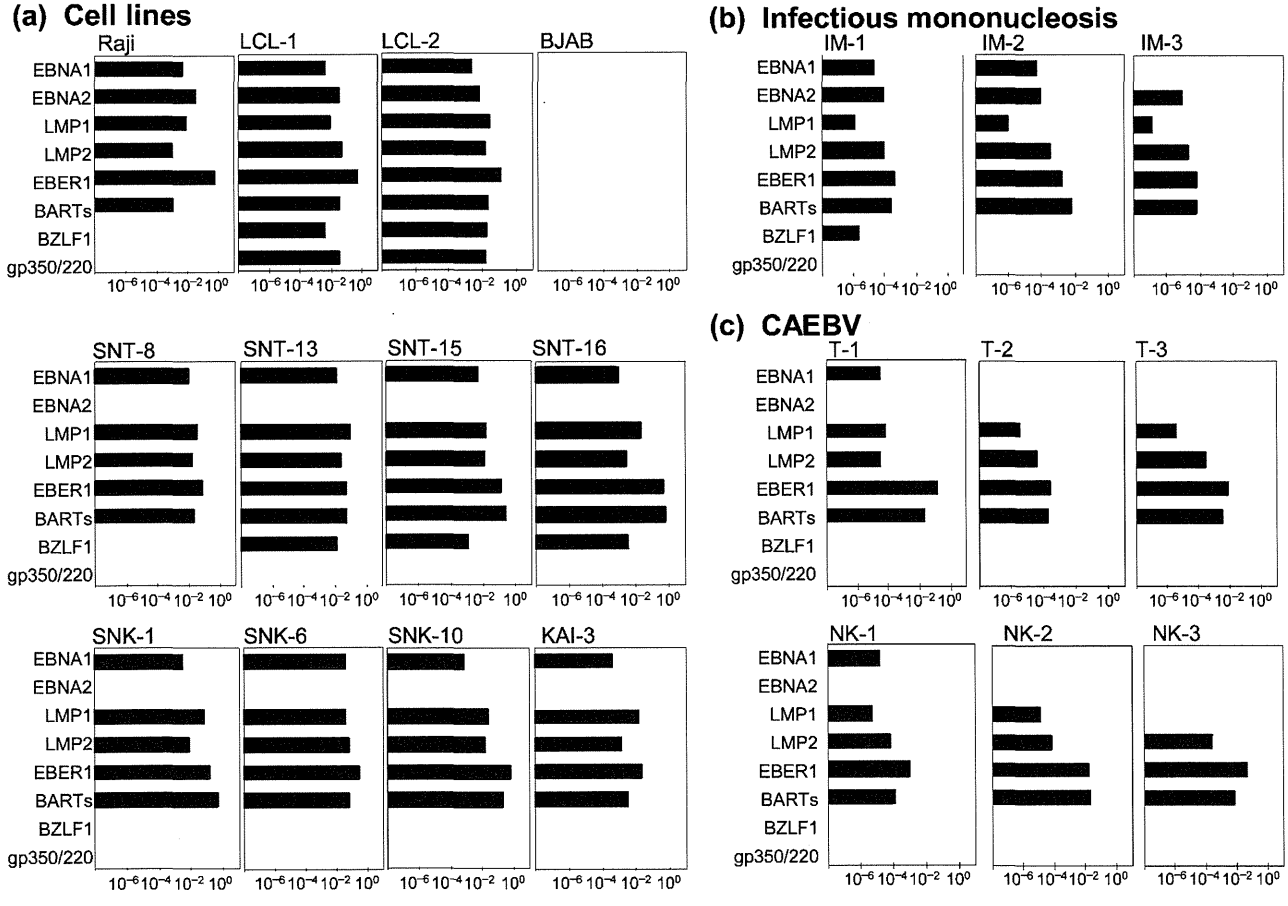

Fig. 1. Analysis of EBV gene expression by real-time RT-PCR. β2-Microglobin (β2 m) was used as an endogenous control and reference gene for relative quantification and was assigned an arbitrary value of 1 (10^0). (a) The quantity of each EBV gene in B, T and NK cells. Raji, LCL-1 and LCL-2 are EBV-positive B cell lines. BJAB is an EBV-negative B cell line. SNT-8, -13, -15 and -16 are EBV-positive T cell lines. SNK-1, -6, -10 and KAI-3 are EBV-positive NK cell lines. (b) Quantitative expression of the EBV genes in patients with infectious mononucleosis. (c) Representative results showing the relative expression of EBV genes in patients with a CAEBV infection. T-1, -2 and -3 are T-cell-type cases (patients 6, 9 and 11 in Table 1), while NK-1, -2 and -3 are NK-cell-type cases (patients 14, 15 and 19 in Table 1).

BZLF1 was detected in three of four T-cell lines, while gp350/220 was not detected in any of the cell lines, indicating an abortive lytic cycle. These results are consistent with those from previous reports (Leenman *et al.*, 2004; Tao *et al.*, 1998; Tsuge *et al.*, 1999; Zhang *et al.*, 2003), indicating the reliability of our system. We evaluated the sensitivity for each latent EBV gene using a cell mixture containing 1×10^6 EBV-negative BJAB cells and 10-fold serial dilutions of LCL-1 with latency III. The detection limits for EBNA1, EBNA2, LMP1, LMP2, EBER1 and BARTs were 0.1, 0.1, 0.01, 0.01, 0.001 and 0.01 % of LCL-1 cells, respectively. To evaluate the sensitivity for lytic genes, cell mixtures containing BJAB and Akata cells with a lytic infection, induced by human immunoglobulin G, were used. The detection limits for BZLF1 and gp350/220 were 0.1 % of Akata cells.

Next, we analysed blood from three patients with acute-phase infectious mononucleosis (Fig. 1b). EBNA2, LMP1, LMP2, EBER1 and BARTs were detected in the PBMCs of the patients, whereas EBNA1 was detected in two patients. The gene expression pattern in each case was latency type III. BZLF1 was detected in one patient, whereas gp350/220 was not detected in any patient. Furthermore, we analysed the PBMCs of 23 healthy carriers. Four healthy carriers were positive for EBV DNA. Real-time RT-PCR detected EBER1 and BARTs in the PBMCs of one carrier, while EBER1 alone was detected in a single additional carrier.

We next quantified the expression level of each gene in 24 patients with CAEBV. PBMCs collected at the time of diagnosis or referral were used in the analysis. The expression profiles of each patient are shown in Table 1, while the positive rates for each EBV gene are summarized in Table 2. EBER1 and BARTs were detected in each patient, while LMP2 was detected in most patients. EBNA1 and LMP1 were detected less frequently compared with EBER1 and BARTs ($P<0.0001$ and $P=0.004$, respectively). EBNA2 and the lytic genes BZLF1 and gp350/220 were undetected in all of the patients. Representative

Table 1. Characteristics and EBV gene expression profiles of 24 patients with chronic active EBV infection

ND, Not done. EBNA2, BZLF1 and gp350/220 were not expressed in any samples. EBER1 and BARTs were expressed in all samples.

Patient	Age (years)	Gender	Cell type infected	Viral load*				Disease type†	HSCT	Outcome	Viral load‡	EBV gene expression		
				PBMC	$CD3^+$	$CD19^+$	$CD56^+$					EBNA1	LMP1	LMP2
1	6	M	T	85925	**157196**	32828	62047	I	−	Alive	241000	−	+	+
2	5	M	T	74915	**119024**	12292	**77651**	I	−	Alive	392203	+	−	+
3	25	M	T	10749	**12106**	2742	5739	I	−	Alive	297	−	−	−
4	10	M	T	18308	**23422**	12665	**27106**	I	−	Alive	19363	−	+	+
5	6	M	T	14162	**22559**	1583	1073	A	+	Alive	14162	−	−	+
6	4	F	T	15776	**17312**	5243	4321	A	+	Alive	15776	+	+	+
7	11	M	T	60097	**143852**	23212	6352	A	+	Alive	60097	−	−	+
8	18	F	T/B	93458	**118026**	**174042**	**267078**	A	+	Alive	392734	+	+	+
9	14	F	T	30633	**32730**	8345	4760	I	+	Alive	30633	−	+	+
10	24	F	T	8589	**43469**	2388	**12555**	A	−	Dead	37148	+	−	+
11	23	F	T	5684	**7990**	4200	250	I	+	Dead	2764	−	+	+
12	13	M	T	3176	**3579**	948	839	I	+	Dead	10681	+	+	+
13	16	F	T	52978	**55431**	37536	**84110**	I	+	Dead	52978	−	+	+
14	11	M	NK	370000	31600	100000	**1800000**	I	−	Alive	339589	+	+	+
15	9	M	NK	77884	7428	17083	**89352**	I	−	Alive	89930	−	+	+
16	4	M	NK	74550	11288	18423	**86361**	A	+	Alive	74550	+	+	+
17	5	F	NK	11200	330	3300	**23400**	A	+	Alive	1108	+	+	+
18	3	M	NK	131957	1591	16450	**917500**	I	+	Alive	131957	−	+	+
19	9	M	NK	263429	92057	206565	**425956**	I	+	Alive	263429	−	−	+
20§	26	F	NK	18889	ND	ND	ND	I	+	Alive	18889	−	+	−
21	14	F	NK	1559	53	105	**4302**	A	−	Dead	1051	−	−	−
22	14	F	NK	20126	3288	1866	**35252**	I	+	Dead	44750	+	+	+
23§	16	M	NK	69121	ND	ND	ND	I	+	Dead	69121	+	+	+
24§	14	F	NK	1041	ND	ND	ND	I	+	Dead	1041	−	−	−

*Bold type indicates that EBV DNA was concentrated by fractionation; copies $(\mu g\ DNA)^{-1}$.

†Patients with severe symptoms were defined as having a clinically active disease (A); patients with no symptoms or with only skin symptoms were defined as having an inactive disease (I).

‡Indicates the EBV DNA in the PBMCs used for real-time RT-PCR analysis; copies $(\mu g\ DNA)^{-1}$.

§Infection was confirmed by *in situ* hybridization with EBER using fractionated cells.

Table 2. Detection of eight EBV-related genes in 24 patients with a CAEBV infection

Gene	No. positive patients (%)	*P*-value*
EBNA1	10 (42)	<0.001
EBNA2	0 (0)	<0.001
LMP1	16 (67)	0.004
LMP2	20 (83)	0.11
EBER1	24 (100)	–
BARTs	24 (100)	–
BZLF1	0 (0)	<0.001
gp350/220	0 (0)	<0.001

*Comparison with EBER1 and BARTs. All *P*-values were obtained using Fisher's exact test.

quantitative results for each EBV gene are shown in Fig. 1(c).

The negative results obtained for EBNA1 and LMP1 raise the possibility that the test was not sensitive enough to detect low levels of expression. Therefore, we examined the correlation between the relative expression level for each gene and the EBV DNA load in the PBMCs (Fig. 2). For all of the EBV genes examined, the expression level correlated with the EBV DNA load. However, the samples with a low EBV DNA load were not always negative for EBNA1; similar findings were seen for LMP1.

To confirm the EBV gene expression profiles in various cell populations, we separated $CD3^+$, $CD19^+$ and $CD56^+$ cells from the PBMCs by immunomagnetic sorting and quantified the gene expression in each population by real-time RT-PCR using selected patients and healthy carriers. In one patient with T-cell-type CAEBV (patient 2 in Table 1; $CD3^+$ $CD56^+$ T cells harboured EBV), type II latent genes, such as EBNA1, LMP2, EBER1 and BARTs, were detected in both the $CD3^+$ and $CD56^+$ cell populations (Fig. 3a). In a patient with NK-cell-type CAEBV (patient 14 in Table 1), type II latent genes were detected primarily in the $CD56^+$ population (Fig. 3b). On the other hand, in a healthy carrier, EBER1 and BARTs were detected in the $CD19^+$ population (presumed to be the B-cell fraction; Fig. 3c). Importantly, the gene expression profiles in the mainly infected cells largely corresponded to those in the unsorted PBMCs in all three cases, suggesting that our PBMC data could be applied to the cells in the mainly infected population.

We next estimated the mean expression level for each EBV gene in 24 patients with CAEBV (Fig. 4a). EBER1 had the highest relative expression level, followed by BARTs, LMP2 and EBNA1, whereas LMP1 had the lowest. Next, we compared the expression level for each EBV gene between the T- and NK-cell types of CAEBV (Fig. 4b). No significant difference was found, although LMP2 expression tended to be higher in the T-cell type ($P=0.09$). We also compared the expression levels between the clinically active patients, who presented with severe symptoms at the time of sample collection, and clinically inactive patients (Fig. 4c). EBNA1 expression was 8.3 times higher in the active patients than in the inactive patients ($P=0.02$). Additionally, the rate of EBNA1-positive patients in the active group was significantly higher (75 versus 25 %; $P=0.03$). On the other hand, there was no difference in EBV DNA load in the peripheral blood between the active and inactive groups [$10^{4.4}$ versus $10^{4.5}$ copies $(\mu g\ DNA)^{-1}$; $P=0.85$]. We also investigated whether EBV gene expression at the time of diagnosis or referral to our hospital was associated with the subsequent disease outcome. We divided the patients into three groups: survivors without HSCT, survivors with HSCT and non-survivors. No significant difference was observed in the gene expression profiles of the three groups (Fig. 4d).

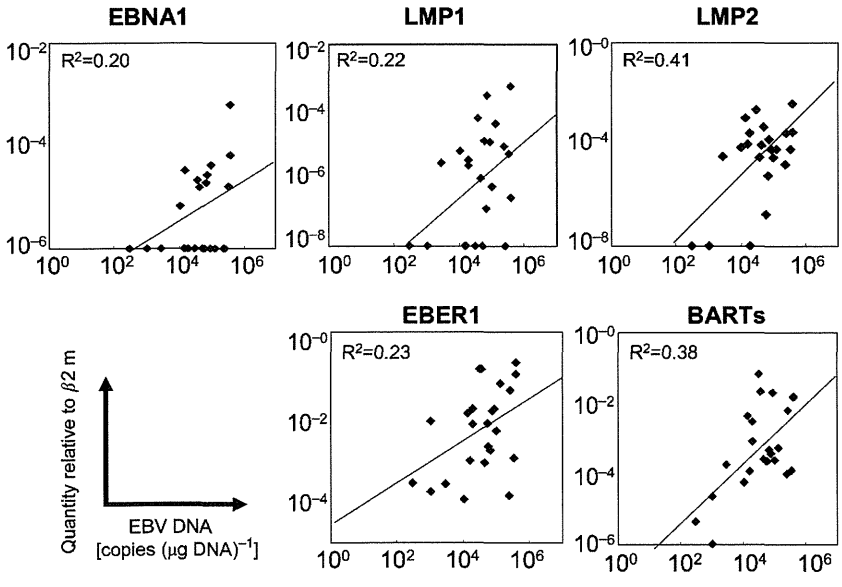

Fig. 2. Relationship between the quantity of each EBV gene and the EBV DNA load in PBMCs from patients with CAEBV. The correlation in all of these was statistically significant.

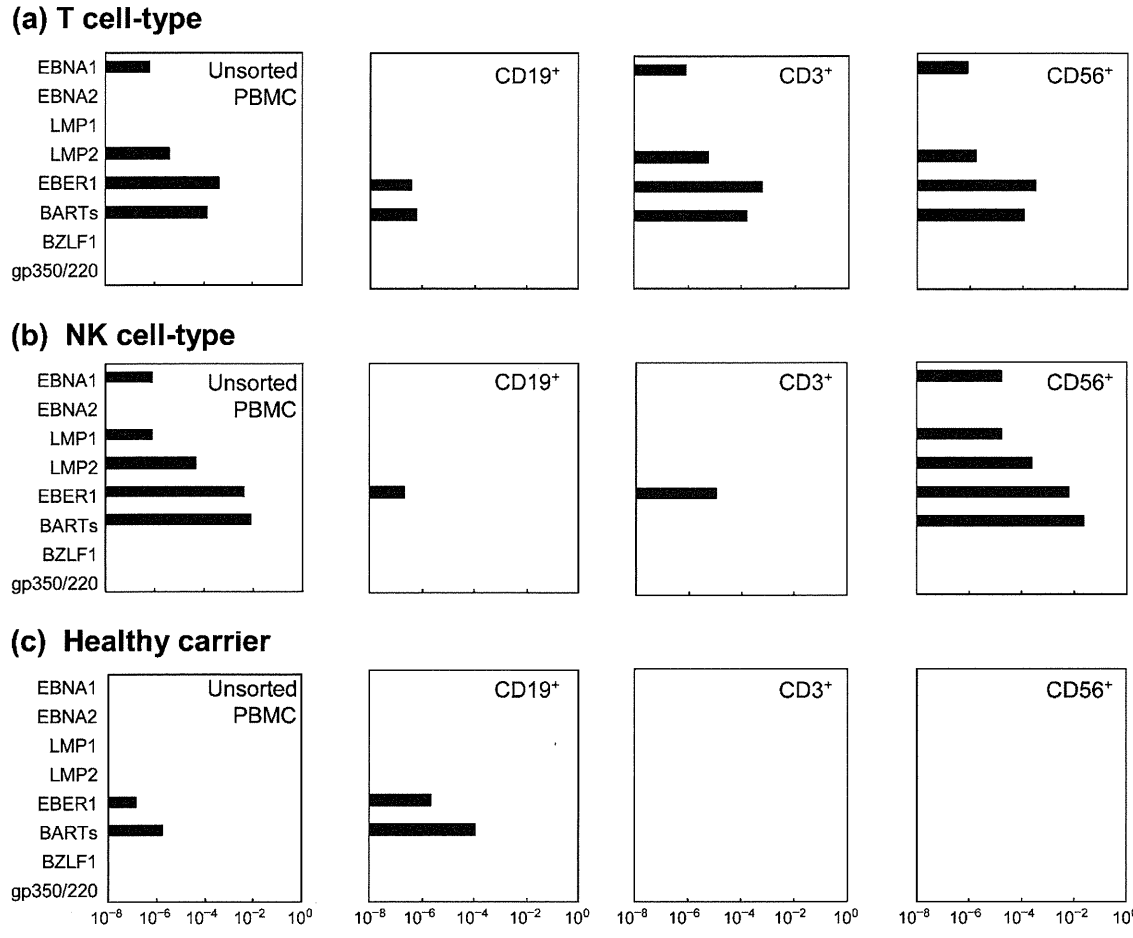

Fig. 3. EBV gene expression in sorted cell populations. CD19$^+$, CD3$^+$ and CD56$^+$ cells were separated by immunomagnetic sorting and analysed by real-time RT-PCR; unsorted PBMCs were analysed. (a) A T-cell-type CAEBV patient (patient 2 in Table 1; CD3$^+$ CD56$^+$ T cells were the main type of infected cells). (b) An NK-cell-type CAEBV patient (patient 14 in Table 1). (c) A healthy carrier whose PBMCs were positive for EBV DNA.

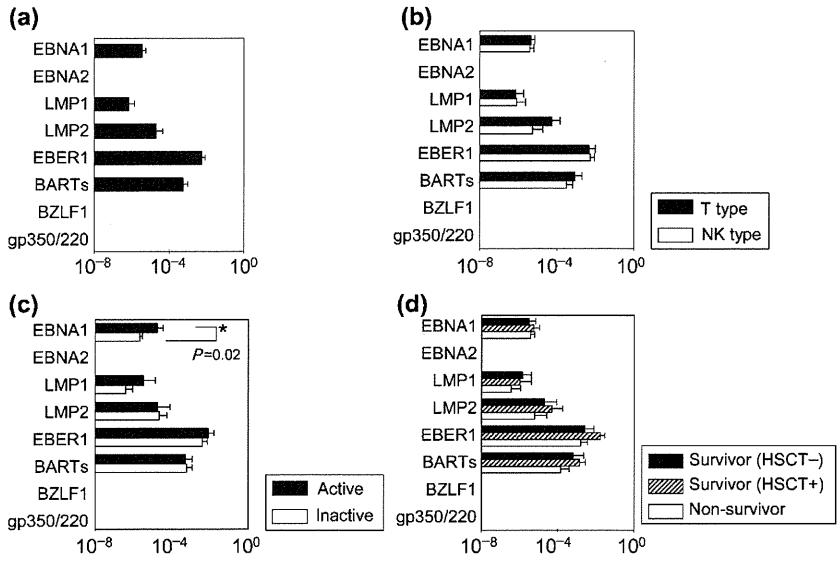

Fig. 4. EBV gene expression profile for patients with CAEBV. The quantity of each EBV gene was analysed by real-time RT-PCR and compared with the β2 m level; the mean ± SE (boxes and bars) was calculated for each gene. (a) Average expression of EBV genes in 24 patients with CAEBV. (b) Comparison between T- (13 cases) and NK- (11 cases) cell-types. (c) Comparison between clinically active (8 cases) and inactive (16 cases) patients. (d) Comparisons of surviving patients without HSCT (6 cases), surviving patients with HSCT (10 cases) and non-surviving patients (8 cases). The Mann–Whitney *U*-test was used to compare the expression values between the groups, while the analysis of variance was used to compare the groups of three.

Finally, to eliminate any potential influence of therapeutic interventions, we excluded six patients who had received therapy before entering our hospital and re-evaluated the expression of each gene in the remaining 18 patients. The level of EBNA1 expression in the active patients was 8.2 times higher than that in the inactive patients ($P=0.03$) and the rate of EBNA1-positive patients was significantly higher in the active group (83 versus 25 %; $P=0.04$). We also re-evaluated the disease outcome in these 18 patients. No significant difference was observed in the gene expression profiles between the three groups according to outcome (data not shown).

DISCUSSION

Analysing the expression profile of EBV-related genes is essential to clarify the pathogenesis of EBV-associated diseases and to uncover information regarding the prognosis of individual patients and potential therapeutic interventions. In recent years, a quantitative method for the analysis of EBV gene expression has been applied to infectious mononucleosis (Weinberger *et al.*, 2004), Burkitt's lymphoma and nasopharyngeal carcinoma (Bell *et al.*, 2006). In the present study, we quantified the expression of six latent genes and two lytic genes in 24 patients with CAEBV using one-step multiplex real-time RT-PCR. To our knowledge, this is the first study to quantify EBV gene expression in CAEBV patients. EBNA1, LMP1, LMP2, EBER1 and BARTs were detected in the patient samples, whereas EBNA2 and the two lytic genes were not detected. The gene expression pattern was latency type II, consistent with previous qualitative RT-PCR results (Kimura *et al.*, 2005). Because the lytic genes BZLF1 and gp350/220 were undetected, a lytic infection is unlikely in the peripheral blood of the CAEBV patients. EBER1 and BARTs were detected in abundance in all patients, while LMP2 was found in most patients. EBNA1 and LMP1 were less frequently detected and had lower expression levels than EBER1 and BARTs. These results are in contrast with similar analyses using T or NK cell lines, in which EBNA1, LMP1, LMP2, EBER1 and BARTs were abundantly and comparably expressed. EBNA1, EBNA2 and EBNA3C are the dominant targets of $CD4^+$ T-cell responses, while EBNA3A, EBNA3B and EBNA3C are the dominant targets of $CD8^+$ T-cell responses (Hislop *et al.*, 2007). In those patients with CAEBV, most or all of these antigens were not expressed, contributing to the evasion of cellular immunity. The decreased frequency and low expression level of EBNA1 may also contribute to the immunological escape mechanism of CAEBV.

The expression profile identified in this study may be useful for obtaining information regarding potential immunotherapies. The EBV-related antigens expressed by infected cells are possible targets for treatment with EBV-specific CTLs. Several studies have reported the use of such therapies for CAEBV, but most have shown only limited effectiveness (Hagihara *et al.*, 2003; Kuzushima *et al.*, 1996; Savoldo *et al.*, 2002). These studies used EBV-specific CTLs that were generated from LCL and targeted latency type III antigens. Our results indicate that EBER1 and BARTs were the most frequently and abundantly expressed EBV genes, followed by LMP2. Because very little EBER1 and BARTs mRNA is translated into protein (Arrand & Rymo, 1982; Kieff & Rickinson, 2007), LMP2 would be the most favourable target for CTL therapy against CAEBV. Recently, EBV-specific CTLs targeted against LMP2 were used to treat Hodgkin's lymphoma and nasopharyngeal carcinoma, both of which are latency type II infections (Bollard *et al.*, 2004, 2007; Straathof *et al.*, 2005). Furthermore, patients with CAEBV generally lack LMP2-specific CTLs (Sugaya *et al.*, 2004). However, to develop effective and useful forms of immunotherapy, additional studies focusing on the nature of the infected cells and the underlying pathology of CAEBV are necessary.

In this study, we quantified the relative expression of EBV latent and lytic genes by real-time RT-PCR. There are a few drawbacks to our system. Firstly, we used β2-microglobulin (β2 m) as a reference for relative quantification; however, comparisons of the levels of expression between different genes may be compromised by variations in the efficiency of the primers used. Another option for such quantification is preparing a standard curve for each cDNA by diluting the plasmid and estimating the number of RNA copies to quantify the expression of each gene more accurately. Secondly, we determined the type of latency based on the patterns of viral gene expression. Promoter usage for EBNA1 is different between latency types I/II and III (Qp versus Cp) (Kieff & Rickinson, 2007). Primers capable of distinguishing between the two EBNA1 promoters would enable us to confirm the type of latency more accurately. Bell *et al.* (2006) used such a system to distinguish latency types and quantify gene expression using different EBNA1 primers.

There are several possible reasons why EBNA1 and LMP1 were detected less frequently in our analysis. First, EBV-infected T or NK cells in some patients with CAEBV may indeed express very little LMP1 or EBNA1. A previous experiment performed using nested RT-PCR, which is sensitive but not quantitative, showed that these genes were expressed in less than half of CAEBV patients (Kimura *et al.*, 2005). Second, the sensitivity of the test may be too low to detect these genes. However, those samples with a low EBV DNA load in this study were not always negative for EBNA1 or LMP1, indicating that low sensitivity was not the only reason that the expression of these genes was not detected. Moreover, EBV polymorphisms may have affected our results. Indeed, the primers used for LMP1 are specific for polymorphic regions (Kubota *et al.*, 2008). However, we used mixed primers for LMP1 to account for sequence variations, and the EBNA1 primers were designed to recognize fairly conserved regions. Furthermore, we also examined EBNA1- or LMP1-negative samples by nested RT-PCR using alternate primer sets (Kimura *et al.*, 2005).

Neither EBNA1 nor LMP1 was detected in any of the samples by nested PCR (data not shown).

EBNA1 was detected more frequently and abundantly in the clinically active patients. EBNA1 is the only EBV protein consistently expressed in all proliferating cells, and it plays central roles in the maintenance and replication of the episomal EBV genome. EBNA1 also has a role in cell growth and survival (Kieff & Rickinson, 2007; Thorley-Lawson & Gross, 2004). Recently, Saridakis *et al.* (2005) demonstrated that EBNA1 inhibits apoptosis by binding to USP7, which destabilizes p53. Together with our results, these findings suggest that EBNA1 plays an important part in the pathogenesis and symptoms of CAEBV.

EBV gene expression has been shown to be related to the prognosis of EBV-associated diseases. Kwon *et al.* (2006) evaluated EBER and LMP1 expression in patients with Hodgkin's lymphoma, while Tsang *et al.* (2003) reported a relationship between the recurrence and detection of LMP1 in patients with nasopharyngeal carcinoma. Similarly, we evaluated the relationship between EBV gene expression and the prognosis of CAEBV, but were unable to identify a significant link. Other factors that may have influenced the results of this study include the small sample size, short observation period and therapeutic interventions such as HSCT. Additional studies with a greater number of cases and a longer observation period are necessary to reach conclusions about the prognostic value of EBV gene quantification for CAEBV. In conclusion, we applied a real-time RT-PCR system to PBMCs from patients with CAEBV and identified the expression profiles of several EBV genes. Quantifying EBV gene expression may be useful in clarifying CAEBV pathogenesis and provide further information about therapeutic interventions, such as CTL therapy.

METHODS

Cell lines. The EBV-positive B cell lines used in this study were Raji, Akata, lymphoblastoid cell line (LCL)-1 and LCL-2. BJAB, an EBV-negative B cell line, was used as a negative control. The EBV-positive T cell lines used were SNT-8, -13, -15 and -16 (Zhang *et al.*, 2003). The EBV-positive NK cell lines used were SNK-1, -6 and -10 (Zhang *et al.*, 2003) and KAI-3 (Tsuge *et al.*, 1999). The T/NK cell lines were derived from patients with CAEBV or nasal NK-/T-cell lymphomas.

Patients. Twenty-four patients (13 males and 11 females) with CAEBV, ranging in age from 3 to 26 years (median age 13 years), were enrolled in this study (Table 1). Each patient met the following diagnostic criteria: EBV-related symptoms for at least 6 months (e.g. fever, persistent hepatitis, extensive lymphadenopathy, hepatosplenomegaly, pancytopenia, uveitis, interstitial pneumonia, hydroa vacciniforme or hypersensitivity to mosquito bites), an increased EBV load in either the affected tissue or peripheral blood, and no evidence of previous immunological abnormalities or other recent infections that could explain the condition (Kimura, 2006; Kimura *et al.*, 2001). Based on the infected cell type, 13 patients were identified as having T-cell-type CAEBV, while 11 were identified as having NK-cell-type CAEBV. To determine which cells harboured the most EBV, peripheral blood mononuclear cells (PBMCs) were fractionated into $CD3^+$, $CD19^+$ and $CD56^+$ cells and analysed by either quantitative PCR or *in situ* hybridization, using EBER1 as a probe, as described previously (Kimura *et al.*, 2001, 2005). The patients were defined as having a T-cell-type infection if their $CD3^+$ cells contained larger amounts of EBV DNA than their PBMCs, or if their $CD3^+$ cells gave a positive hybridization signal with EBER1. The patients were defined as having an NK-cell-type infection if their $CD56^+$ cells, rather than their $CD3^+$ cells, were the major cells harbouring EBV. The EBV DNA copy numbers in each cell population are shown in Table 1.

Peripheral blood was collected at the time of diagnosis or referral to our hospital. Six of 24 patients had already received steroid therapy or chemotherapy. PBMCs were isolated using Ficoll–Paque density gradients (Pharmacia Biotech) and stored at −80 °C until further use. Eight patients with severe symptoms such as high fever, distinct hepatosplenomegaly, and/or elevated hepatic transaminase levels at the time of sample collection were defined as having clinically active disease, while 16 patients with no symptoms or with only skin symptoms, including hydroa vacciniforme, were defined as having inactive disease. Eight of the patients died after 1–49 months of observation (median 14 months). Sixteen of the patients, 10 of whom received HSCT, were alive after 9–115 months of observation (median 28 months). Twenty-three healthy carrier volunteers who were seropositive for EBV and three patients with infectious mononucleosis (aged 5, 11 and 29 years) were enrolled as controls.

Informed consent was obtained from all patients or their guardians. The institutional review board of Nagoya University Hospital approved the use of the specimens that were examined in this study.

Real-time PCR assay. DNA was extracted from 1×10^6 PBMCs using a QIAmp blood mini kit (Qiagen). EBV DNA was quantified by real-time PCR as described previously. The viral load is expressed as the number of copies $(\mu g\ DNA)^{-1}$ (Kimura *et al.*, 1999).

RNA was extracted from 1×10^6 cells using a QIAmp RNeasy mini kit (Qiagen). Contaminating DNA was removed by on-column DNase digestion using the RNase-free DNase set (Qiagen) (Kubota *et al.*, 2008). Viral mRNA expression was quantified by one-step multiplex real-time RT-PCR using an Mx3000P real-time PCR system (Stratagene) as described previously (Kubota *et al.*, 2008). All of the primer/probe combinations, except those for EBER1 lacking an intron, were designed to span introns to avoid amplifying residual genomic DNA. The primer and probe sequences are listed in Supplementary Table S1 (available in JGV Online). The primers used for EBNA1, EBNA2, LMP1 and BZLF1, which were described previously (Kubota *et al.*, 2008), were modified according to sequence variations amongst the strains. The stably expressed housekeeping gene $\beta 2$ m was used as an endogenous control and reference gene for relative quantification (Patel *et al.*, 2004).

Cell sorting and gene expression analysis. $CD3^+$, $CD19^+$ and $CD56^+$ cells were separated from 1×10^7 PBMCs by immunomagnetic sorting using anti-CD3, -CD19 and -CD56 MACS Microbeads, respectively (Miltenyi Biotec). After two rounds of sorting, the purity of the populations exceeded 95 %. RNA was extracted from each cell population for real-time RT-PCR analysis. For comparison, RNA was also extracted from unsorted PBMCs.

Statistical analyses. All statistical analyses were performed using StatView (version 5.0; SAS Institute). Geometric (logarithmic) means were calculated for the expression of each EBV gene. For the negative samples, the default value, which was defined as the lowest level of expression for a particular gene, was used for the calculation. The default values for the undetected genes EBNA1, LMP1 and LMP2 were 10^{-6}, 10^{-8} and 10^{-8}, respectively. The Mann–Whitney *U*-test was used to compare the expression levels between groups, while analysis of variance was used to compare three groups. Fisher's exact

test was used to compare positive rates of gene expression. A regression analysis was used to compare the expression of each gene and the EBV DNA load. *P*-values <0.05 were deemed to be statistically significant.

ACKNOWLEDGEMENTS

We thank the following people for their contributions to this study: Kayoko Matsunaga (Fujita Health University); Masaki Ito, Atsushi Kikuta, and Mitsuaki Hosoya (Fukushima Medical University); Tomohiro Kinoshita (Nagoya University); Kazuhiko Shirota (National Hospital Organization Shizuoka Medical Center); Mariko Seishima (Ogaki Municipal Hispital); Masashi Shiomi (Osaka City General Hospital); Hajime Katsumata and Yasuo Horikoshi (Shizuoka Children's Hospital); Tsuyoshi Ito (Toyohashi City Hospital); and Sachiyo Kamimura (University of Miyazaki). This study was supported in part by a grant from the Ministry of Education, Culture, Sports, Science and Technology, Japan (19591247).

REFERENCES

Arrand, J. R. & Rymo, L. (1982). Characterization of the major Epstein–Barr virus-specific RNA in Burkitt lymphoma-derived cells. *J Virol* **41**, 376–389.

Bell, A. I., Groves, K., Kelly, G. L., Croom-Carter, D., Hui, E., Chan, A. T. & Rickinson, A. B. (2006). Analysis of Epstein–Barr virus latent gene expression in endemic Burkitt's lymphoma and nasopharyngeal carcinoma tumour cells by using quantitative real-time PCR assays. *J Gen Virol* **87**, 2885–2890.

Bollard, C. M., Aguilar, L., Straathof, K. C., Gahn, B., Huls, M. H., Rousseau, A., Sixbey, J., Gresik, M. V., Carrum, G. & other authors (2004). Cytotoxic T lymphocyte therapy for Epstein–Barr virus^{+} Hodgkin's disease. *J Exp Med* **200**, 1623–1633.

Bollard, C. M., Gottschalk, S., Leen, A. M., Weiss, H., Straathof, K. C., Carrum, G., Khalil, M., Wu, M. F., Huls, M. H. & other authors (2007). Complete responses of relapsed lymphoma following genetic modification of tumor-antigen presenting cells and T-lymphocyte transfer. *Blood* **110**, 2838–2845.

Brooks, L., Yao, Q. Y., Rickinson, A. B. & Young, L. S. (1992). Epstein–Barr virus latent gene transcription in nasopharyngeal carcinoma cells: coexpression of EBNA1, LMP1, and LMP2 transcripts. *J Virol* **66**, 2689–2697.

Cohen, J. I. (2000). Epstein–Barr virus infection. *N Engl J Med* **343**, 481–492.

Deacon, E. M., Pallesen, G., Niedobitek, G., Crocker, J., Brooks, L., Rickinson, A. B. & Young, L. S. (1993). Epstein–Barr virus and Hodgkin's disease: transcriptional analysis of virus latency in the malignant cells. *J Exp Med* **177**, 339–349.

Fujii, N., Takenaka, K., Hiraki, A., Maeda, Y., Ikeda, K., Shinagawa, K., Ashiba, A., Munemasa, M., Sunami, K. & other authors (2000). Allogeneic peripheral blood stem cell transplantation for the treatment of chronic active Epstein-Barr virus infection. *Bone Marrow Transplant* **26**, 805–808.

Gotoh, K., Ito, Y., Shibata-Watanabe, Y., Kawada, J., Takahashi, Y., Yagasaki, H., Kojima, S., Nishiyama, Y. & Kimura, H. (2008). Clinical and virological characteristics of 15 patients with chronic active Epstein–Barr virus infection treated with hematopoietic stem cell transplantation. *Clin Infect Dis* **46**, 1525–1534.

Hagihara, M., Tsuchiya, T., Hyodo, O., Ueda, Y., Tazume, K., Masui, A., Kanemura, A., Yoshiba, F., Takashimizu, S. & other authors (2003). Clinical effects of infusing anti-Epstein–Barr virus (EBV)-specific cytotoxic T-lymphocytes into patients with severe chronic active EBV infection. *Int J Hematol* **78**, 62–68.

Heslop, H. E., Ng, C. Y., Li, C., Smith, C. A., Loftin, S. K., Krance, R. A., Brenner, M. K. & Rooney, C. M. (1996). Long-term restoration of immunity against Epstein–Barr virus infection by adoptive transfer of gene-modified virus-specific T lymphocytes. *Nat Med* **2**, 551–555.

Hislop, A. D., Taylor, G. S., Sauce, D. & Rickinson, A. B. (2007). Cellular responses to viral infection in humans: lessons from Epstein–Barr virus. *Annu Rev Immunol* **25**, 587–617.

Kanegane, H., Nomura, K., Miyawaki, T. & Tosato, G. (2002). Biological aspects of Epstein–Barr virus (EBV)-infected lymphocytes in chronic active EBV infection and associated malignancies. *Crit Rev Oncol Hematol* **44**, 239–249.

Kieff, E. D. & Rickinson, A. V. (2007). Epstein–Barr virus and its replication. In *Fields Virology*, pp. 2603–2654. Edited by D. M. Knipe & P. M. Howley. Philadelphia: Lippincott Williams & Wilkins.

Kimura, H. (2006). Pathogenesis of chronic active Epstein–Barr virus infection: is this an infectious disease, lymphoproliferative disorder, or immunodeficiency? *Rev Med Virol* **16**, 251–261.

Kimura, H., Morita, M., Yabuta, Y., Kuzushima, K., Kato, K., Kojima, S., Matsuyama, T. & Morishima, T. (1999). Quantitative analysis of Epstein–Barr virus load by using a real-time PCR assay. *J Clin Microbiol* **37**, 132–136.

Kimura, H., Hoshino, Y., Kanegane, H., Tsuge, I., Okamura, T., Kawa, K. & Morishima, T. (2001). Clinical and virologic characteristics of chronic active Epstein-Barr virus infection. *Blood* **98**, 280–286.

Kimura, H., Morishima, T., Kanegane, H., Ohga, S., Hoshino, Y., Maeda, A., Imai, S., Okano, M., Morio, T. & other authors (2003). Prognostic factors for chronic active Epstein–Barr virus infection. *J Infect Dis* **187**, 527–533.

Kimura, H., Hoshino, Y., Hara, S., Sugaya, N., Kawada, J., Shibata, Y., Kojima, S., Nagasaka, T., Kuzushima, K. & Morishima, T. (2005). Differences between T cell-type and natural killer cell-type chronic active Epstein–Barr virus infection. *J Infect Dis* **191**, 531–539.

Kubota, N., Wada, K., Ito, Y., Shimoyama, Y., Nakamura, S., Nishiyama, Y. & Kimura, H. (2008). One-step multiplex real-time PCR assay to analyse the latency patterns of Epstein–Barr virus infection. *J Virol Methods* **147**, 26–36.

Kuzushima, K., Yamamoto, M., Kimura, H., Ando, Y., Kudo, T., Tsuge, I. & Morishima, T. (1996). Establishment of anti-Epstein–Barr virus (EBV) cellular immunity by adoptive transfer of virus-specific cytotoxic T lymphocytes from an HLA-matched sibling to a patient with severe chronic active EBV infection. *Clin Exp Immunol* **103**, 192–198.

Kwon, J. M., Park, Y. H., Kang, J. H., Kim, K., Ko, Y. H., Ryoo, B. Y., Lee, S. S., Lee, S. I., Koo, H. H. & Kim, W. S. (2006). The effect of Epstein–Barr virus status on clinical outcome in Hodgkin's lymphoma. *Ann Hematol* **85**, 463–468.

Leenman, E. E., Panzer-Grumayer, R. E., Fischer, S., Leitch, H. A., Horsman, D. E., Lion, T., Gadner, H., Ambros, P. F. & Lestou, V. S. (2004). Rapid determination of Epstein–Barr virus latent or lytic infection in single human cells using *in situ* hybridization. *Mod Pathol* **17**, 1564–1572.

Okamura, T., Hatsukawa, Y., Arai, H., Inoue, M. & Kawa, K. (2000). Blood stem-cell transplantation for chronic active Epstein–Barr virus with lymphoproliferation. *Lancet* **356**, 223–224.

Okano, M., Kawa, K., Kimura, H., Yachie, A., Wakiguchi, H., Maeda, A., Imai, S., Ohga, S., Kanegane, H. & other authors (2005). Proposed guidelines for diagnosing chronic active Epstein–Barr virus infection. *Am J Hematol* **80**, 64–69.

Patel, K., Whelan, P. J., Prescott, S., Brownhill, S. C., Johnston, C. F., Selby, P. J. & Burchill, S. A. (2004). The use of real-time reverse

transcription-PCR for prostate-specific antigen mRNA to discriminate between blood samples from healthy volunteers and from patients with metastatic prostate cancer. *Clin Cancer Res* **10**, 7511–7519.

Quintanilla-Martinez, L., Kumar, S., Fend, F., Reyes, E., Teruya-Feldstein, J., Kingma, D. W., Sorbara, L., Raffeld, M., Straus, S. E. & Jaffe, E. S. (2000). Fulminant EBV(+) T-cell lymphoproliferative disorder following acute/chronic EBV infection: a distinct clinicopathologic syndrome. *Blood* **96**, 443–451.

Rickinson, A. B. & Kieff, E. (2007). Epstein–Barr virus. In *Fields Virology*, pp. 2655–2700. Edited by D. M. Knipe & P. M. Howley. Philadelphia: Lippincott Williams & Wilkins.

Rooney, C. M., Smith, C. A., Ng, C. Y., Loftin, S. K., Sixbey, J. W., Gan, Y., Srivastava, D. K., Bowman, L. C., Krance, R. A. & other authors (1998). Infusion of cytotoxic T cells for the prevention and treatment of Epstein–Barr virus-induced lymphoma in allogeneic transplant recipients. *Blood* **92**, 1549–1555.

Saridakis, V., Sheng, Y., Sarkari, F., Holowaty, M. N., Shire, K., Nguyen, T., Zhang, R. G., Liao, J., Lee, W. & other authors (2005). Structure of the p53 binding domain of HAUSP/USP7 bound to Epstein–Barr nuclear antigen 1 implications for EBV-mediated immortalization. *Mol Cell* **18**, 25–36.

Savoldo, B., Huls, M. H., Liu, Z., Okamura, T., Volk, H. D., Reinke, P., Sabat, R., Babel, N., Jones, J. F. & other authors (2002). Autologous Epstein–Barr virus (EBV)-specific cytotoxic T cells for the treatment of persistent active EBV infection. *Blood* **100**, 4059–4066.

Straathof, K. C., Leen, A. M., Buza, E. L., Taylor, G., Huls, M. H., Heslop, H. E., Rooney, C. M. & Bollard, C. M. (2005). Characterization of latent membrane protein 2 specificity in CTL lines from patients with EBV-positive nasopharyngeal carcinoma and lymphoma. *J Immunol* **175**, 4137–4147.

Straus, S. E. (1988). The chronic mononucleosis syndrome. *J Infect Dis* **157**, 405–412.

Sugaya, N., Kimura, H., Hara, S., Hoshino, Y., Kojima, S., Morishima, T., Tsurumi, T. & Kuzushima, K. (2004). Quantitative analysis of Epstein–Barr virus (EBV)-specific $CD8^+$ T cells in patients with chronic active EBV infection. *J Infect Dis* **190**, 985–988.

Taketani, T., Kikuchi, A., Inatomi, J., Hanada, R., Kawaguchi, H., Ida, K., Oh-Ishi, T., Arai, T., Kishimoto, H. & Yamamoto, K. (2002). Chronic active Epstein–Barr virus infection (CAEBV) successfully treated with allogeneic peripheral blood stem cell transplantation. *Bone Marrow Transplant* **29**, 531–533.

Tao, Q., Robertson, K. D., Manns, A., Hildesheim, A. & Ambinder, R. F. (1998). Epstein–Barr virus (EBV) in endemic Burkitt's lymphoma: molecular analysis of primary tumor tissue. *Blood* **91**, 1373–1381.

Thorley-Lawson, D. A. & Gross, A. (2004). Persistence of the Epstein–Barr virus and the origins of associated lymphomas. *N Engl J Med* **350**, 1328–1337.

Tosato, G., Straus, S., Henle, W., Pike, S. E. & Blaese, R. M. (1985). Characteristic T cell dysfunction in patients with chronic active Epstein–Barr virus infection (chronic infectious mononucleosis). *J Immunol* **134**, 3082–3088.

Tsang, N. M., Chuang, C. C., Tseng, C. K., Hao, S. P., Kuo, T. T., Lin, C. Y. & Pai, P. C. (2003). Presence of the latent membrane protein 1 gene in nasopharyngeal swabs from patients with mucosal recurrent nasopharyngeal carcinoma. *Cancer* **98**, 2385–2392.

Tsuge, I., Morishima, T., Morita, M., Kimura, H., Kuzushima, K. & Matsuoka, H. (1999). Characterization of Epstein–Barr virus (EBV)-infected natural killer (NK) cell proliferation in patients with severe mosquito allergy; establishment of an IL-2-dependent NK-like cell line. *Clin Exp Immunol* **115**, 385–392.

Weinberger, B., Plentz, A., Weinberger, K. M., Hahn, J., Holler, E. & Jilg, W. (2004). Quantitation of Epstein–Barr virus mRNA using reverse transcription and real-time PCR. *J Med Virol* **74**, 612–618.

Williams, H. & Crawford, D. H. (2006). Epstein–Barr virus: the impact of scientific advances on clinical practice. *Blood* **107**, 862–869.

Young, L., Alfieri, C., Hennessy, K., Evans, H., O'Hara, C., Anderson, K. C., Ritz, J., Shapiro, R. S., Rickinson, A. & other authors (1989). Expression of Epstein–Barr virus transformation-associated genes in tissues of patients with EBV lymphoproliferative disease. *N Engl J Med* **321**, 1080–1085.

Zhang, Y., Nagata, H., Ikeuchi, T., Mukai, H., Oyoshi, M. K., Demachi, A., Morio, T., Wakiguchi, H., Kimura, N. & other authors (2003). Common cytological and cytogenetic features of Epstein–Barr virus (EBV)-positive natural killer (NK) cells and cell lines derived from patients with nasal T/NK-cell lymphomas, chronic active EBV infection and hydroa vacciniforme-like eruptions. *Br J Haematol* **121**, 805–814.

Journal of Pathology
J Pathol 2010; 221: 164–174
Published online 18 February 2010 in Wiley InterScience
(www.interscience.wiley.com) DOI: 10.1002/path.2699

ORIGINAL PAPER

Interleukin-2 induces NF-κB activation through BCL10 and affects its subcellular localization in natural killer lymphoma cells

Ka-Kui Chan,[1] Lijun Shen,[1] Wing-Yan Au,[2] Hiu-Fung Yuen,[1] Kai-Yau Wong,[1] Tianhuan Guo,[1] Michelle LY Wong,[1] Norio Shimizu,[3] Junjiro Tsuchiyama,[4] Yok-Lam Kwong,[2] Raymond HS Liang[2] and Gopesh Srivastava[1]*

[1] Department of Pathology, The University of Hong Kong, Queen Mary Hospital, Hong Kong, China
[2] Department of Medicine, The University of Hong Kong, Queen Mary Hospital, Hong Kong, China
[3] Medical Research Institute, Tokyo Medical and Dental University, Tokyo, Japan
[4] Department of Pathology, Kawasaki Medical School, Kurashiki, Okayama, Japan

*Correspondence to: Gopesh Srivastava, Lymphoma Research Laboratory, Department of Pathology, The University of Hong Kong, Queen Mary Hospital, Pokfulam, Hong Kong, China. e-mail: gopesh@pathology.hku.hk

Abstract

Deregulation of nuclear factor (NF)-κB signalling is common in cancers and is essential for tumourigenesis. Constitutive NF-κB activation in extranodal natural killer (NK)-cell lymphoma, nasal type (ENKL) is known to be associated with aberrant nuclear translocation of BCL10. Here we investigated the mechanisms leading to NF-κB activation and BCL10 nuclear localization in ENKLs. Given that ENKLs are dependent on T-cell-derived interleukin-2 (IL2) for cytotoxicity and proliferation, we investigated whether IL2 modulates NF-κB activation and BCL10 subcellular localization in ENKLs. In the present study, IL2-activated NK lymphoma cells were found to induce NF-κB activation via the PI3K/Akt pathway, leading to an increase in the entry of G_2/M phase and concomitant transcription of NF-κB-responsive genes. We also found that BCL10, a key mediator of NF-κB signalling, participates in the cytokine receptor-induced activation of NF-κB. Knockdown of BCL10 expression resulted in deficient NF-κB signalling, whereas Akt activation was unaffected. Our results suggest that BCL10 plays a role downstream of Akt in the IL2-triggered NF-κB signalling pathway. Moreover, the addition of IL2 to NK cells led to aberrant nuclear translocation of BCL10, which is a pathological feature of ENKLs. We further show that BCL10 can bind to BCL3, a transcriptional co-activator and nuclear protein. Up-regulation of BCL3 expression was observed in response to IL2. Similar to BCL10, the expression and nuclear translocation of BCL3 were induced by IL2 in an Akt-dependent manner. The nuclear translocation of BCL10 was also dependent on BCL3 because silencing BCL3 by RNA interference abrogated this translocation. We identified a critical role for BCL10 in the cytokine receptor-induced NF-κB signalling pathway, which is essential for NK cell activation. We also revealed the underlying mechanism that controls BCL10 nuclear translocation in NK cells. Our findings provide insight into a molecular network within the NF-κB signalling pathway that promotes the pathogenesis of NK cell lymphomas.

Keywords: NK cell lymphoma; IL2; nucleus; BCL10; NF-κB

Received 21 August 2009; Revised 4 January 2010; Accepted 3 February 2010

No conflicts of interest were declared.

Introduction

Extranodal natural killer (NK)-cell lymphoma, nasal type (ENKL) is a major NK cell malignancy that occurs in Asia and Central and South America. Most cases are of NK cell origin, exhibiting CD56 but lacking surface CD3 expression [1]. Immunohistochemistry shows that the tumour cells display an activated NK cell phenotype, with the expression of various cytolytic lymphocyte-associated proteins and surface markers [2,3]. Previously, we reported that constitutive nuclear factor (NF)-κB activation is present in ENKLs but not in resting normal NK cells [4]. This phenotype was also strongly associated with another specific molecular feature, the nuclear translocation of BCL10 in ENKL cells ($p = 0.001$). The underlying molecular mechanisms of this disease, however, are still elusive.

The *BCL10* gene was originally identified from the recurrent involvement of t(1;14)(p22;q32) in gastric mucosa-associated lymphoid tissue (MALT) lymphoma and encodes a cytosolic protein composed of 233 amino acids with pro-inflammatory activity [5]. Nuclear translocation of BCL10 occurs frequently in MALT lymphomas with t(1;14)(p22;q32) and t(11;18)(q21;q21) [6], resulting in more BCL10 protein in tumour cells via the overexpression or stabilization of the protein [7,8]. ENKLs do not harbour these chromosomal aberrations; thus, it is not likely that the same mechanism accounts for the presence of nuclear BCL10 in ENKLs. An alternative mechanism responsible for the same feature of nuclear translocation of BCL10 in ENKLs must exist.

BCL10 is a molecular adaptor that mediates canonical NF-κB signalling in T and B lymphocytes [9–11]. It forms a signalosome along with CARMA1 and MALT1 to relay the antigen receptor signals that activate IKKγ [12]. When the IKK complex is activated, the NF-κB inhibitor IκBα is degraded and NF-κB is allowed to enter the nucleus to induce the transcription of numerous NF-κB-responsive genes. Recent studies have shown that rather than cytotoxicity, the selective role of BCL10 mediates cytokine production when ITAM-coupled NK cell receptors are engaged [13,14]. In contrast to the well-characterized antigen receptor-induced NF-κB signalling, the role of BCL10 in cytokine receptor signalling remains elusive.

Cytokine deregulation is closely associated with the pathogenesis of haematological diseases and cytokine expression patterns sometimes have diagnostic value [15,16]. Notably, interleukin-2 (IL2) is a potent cytokine that promotes the proliferation of primary NK cells. In addition, most of the NK cell lines derived from ENKL are IL2-dependent [17–19]. It is conceivable that IL2 is a survival factor for tumour cells. Moreover, IL2 can cause NF-κB activation; however, the link between the IL2 receptor and NF-κB is less clearly defined [20]. The signalling pathways triggered by the IL2 receptor are diverse and include the JAK/STAT, PI3K/Akt, and Ras/MAPK pathways [21,22]. Among these, Akt was shown to regulate the induction of NF-κB in Jurkat cells and act as a stimulatory signal triggered by antigen engagement, which involves BCL10 [23,24]. We examined the role of Akt and BCL10 in ENKL cells in the cytokine receptor-triggered signalling cascades. Tumour necrosis factor-α (TNF-α), another cytokine, has been shown to induce BCL10 nuclear localization in breast cancer cells [25], suggesting that cytokine stimulation may be one of the contributing factors to aberrant nuclear BCL10 expression. We investigated the effect of IL2 stimulation on BCL10 subcellular localization in NK lymphoma cells to demonstrate the underlying molecular mechanisms.

Materials and methods

Cell lines and reagents

The human NK cell lines SNK-6 and NK-YS of ENKL origin [26] were maintained in RPMI 1640 medium (Hyclone, Logan, UT, USA) supplemented with 10% fetal bovine serum, 2 mM L-glutamine, 100 U/ml penicillin, and 100 μg/ml streptomycin. The cells were routinely cultured with a supplement of 100 U/ml recombinant human IL2 (PeproTech, London, UK). Before the experiments, both cell lines were starved of IL2 for 48 h and then treated with IL2 for 4 h, unless otherwise specified. Cycloheximide (CHX) and Akt inhibitor I (Akt-I) (Calbiochem, Merck Biosciences, Darmstadt, Germany) were dissolved in ethanol and dimethyl sulphoxide (DMSO), respectively, and added 30 min before the addition of IL2 in some experiments. The antibodies used in the study are described in the Supporting information, Supplementary Table 1.

Isolation of normal NK cells

Normal NK cells were isolated from the peripheral blood of two healthy volunteers using the Dynal® NK Cell Negative Isolation Kit (Dynal Biotech, Oslo, Norway). The purity of the NK cells was verified by flow cytometry and found to be over 95%. The normal NK cells were cultured under the same conditions as those described above for the NK cell lines.

RT-PCR analysis

Total RNA was extracted using TRIzol reagent (Invitrogen, Carlsbad, CA, USA). The first-strand cDNA was synthesized from 2 μg of RNA using oligo $d(T)_{16}$ and the GeneAmp RNA PCR Kit (Applied Biosystems, Foster City, CA, USA). Semi-quantitative RT-PCR was performed to detect granzyme B, perforin, *BCL3*, and *GAPDH* mRNA transcripts using AmpliTaq Gold polymerase (Applied Biosystems). The primers used are described in the Supporting information, Supplementary Table 2. The sequences of the primers used for quantitative RT-PCR for granzyme B, perforin, and actin mRNA transcripts are described in the Supporting information, Supplementary Table 3. Products were stained with SYBR Green (Molecular Probes, Eugene, OR, USA) and analysed using a 7700 Real-Time PCR System (Applied Biosystems).

Yeast two-hybrid screening

Yeast two-hybrid screening was performed using the Matchmaker Two-Hybrid System 3 (Clontech, Mountain View, CA, USA). The cDNA library was generated from the RNA of SNK-6 cells. Small-scale library transformation and screening were performed, and potential positive colonies were analysed by PCR screening and sequencing. Putative interactions were further confirmed by co-immunoprecipitation from the cell lines.

Co-immunoprecipitation and western blotting

Cells were lysed in RIPA buffer (Santa Cruz Biotechnology, Santa Cruz, CA, USA). Protein concentrations were measured using the Bio-Rad DC Protein Assay Kit (Bio-Rad, Hercules, CA, USA). Proteins were immunoprecipitated with antibodies or isotype-matched immunoglobulin at 4 °C overnight. The bound protein–antibody complexes were pulled down with protein G plus-agarose (Santa Cruz Biotechnology). The products were resolved by 10% SDS-PAGE and transferred to a PVDF membrane. The membrane was blocked with 5% non-fat milk and incubated with the primary antibody at 4 °C overnight or at room temperature for 1 h. After washing with TBST, the membrane was incubated with an HRP-conjugated secondary antibody for 1 h at room temperature. Signals were detected using Hyperfilm with ECL plus reagent (Amersham Biosciences, Piscataway, NJ, USA).

Cellular fractionation

Cells were lysed with 10 mM HEPES containing 1.5 mM $MgCl_2$, 10 mM KCl, 0.5 mM DTT, 0.5 mM PMSF, and 0.2% Nonidet P-40 supplemented with a cocktail of protease inhibitors. Lysates were placed on ice for 10 min and separated by centrifugation at 3000 rpm for 10 min. The supernatant was collected as the cytoplasmic fraction and the cell pellet was further lysed with buffer containing 50 mM Tris (pH 8.0), 500 mM NaCl, 5 mM EDTA, 0.5 mM DTT, 0.5 mM PMSF, 1% Nonidet P-40, and protease inhibitors at 4 °C for 30 min. The supernatant was collected as the nuclear fraction following centrifugation at 13 000 rpm for 10 min at 4 °C.

Electromobility shift assay (EMSA)

The NF-κB oligonucleotide consensus probe and gel shift assay system were purchased from Promega (Madison, WI, USA). The oligonucleotide was labelled with [γ-^{32}P]ATP using a T4 polynucleotide kinase and the unincorporated radionucleotides were removed using MicroSpin G25 columns. Cells were harvested and nuclear protein fractions were collected. Equal amounts of nuclear extracts were incubated with the radioactive probe according to the user manual. For the supershift assay, antibodies against p50 or p65 were added to the reaction mixture and incubated at 4 °C for 1 h. The DNA–protein complexes were resolved in a 5% polyacrylamide gel. The gel was then dried and exposed to X-ray film at −70 °C.

RNA interference with shRNA

Complementary oligonucleotides (Supporting information, Supplementary Table 4) were annealed and ligated with the pSIREN-RetroQ vector using the knockout RNAi system (Clontech). A negative control shRNA oligonucleotide against luciferase (shCon) was provided by the RNAi system. Transfection of the packaging cell line, PT67, was performed using FuGene 6 transfection reagent (Roche, Mannheim, Germany). The medium containing the viral particles was collected 2 days after transfection. The supernatant was filtered through a 0.45 μm filter and polybrene (8 μg/ml) (Sigma-Aldrich, St. Louis, MO, USA) was then added. SNK-6 cells were incubated with the virus-containing supernatant for 24 h and the supernatant was replaced with fresh RPMI medium. Infected cells were collected 1 day later.

Flow cytometry

Cells were collected by centrifugation and washed twice with PBS. The cell pellets were fixed overnight with ice-cold 70% ethanol and the cells were then resuspended in PBS containing 200 μg/ml RNase A and 20 μg/ml propidium iodide (Sigma-Aldrich). The samples were examined using a FACS Calibur flow cytometer (BD Bioscience, San Jose, CA, USA) and the Cell Quest program. Proportions of cells in different phases were quantified with ModFit LT software (Verity Software House, Topsham, ME, USA).

Immunofluorescence microscopy

Cells were collected and cytospun onto slides. After fixation with cold methanol, the slides were incubated with the primary antibody at 4 °C overnight. After washing, a fluorescein isothiocyanate (FITC)-conjugated secondary antibody (Chemicon, Temecula, CA, USA) was applied to the slides. Cell nuclei were counterstained with 4′,6-diamidino-2-phenylindole (DAPI; Roche) and signals were visualized using an Eclipse E800M microscope (Nikon, Tokyo, Japan).

Statistics

The data were compared using the t-test and $p < 0.05$ was regarded to be statistically significant.

Results

IL2 induces NF-κB activation via Akt

To determine whether PI3K and Akt were engaged in IL2-induced NF-κB signalling, two bona fide ENKL cell lines, SNK-6 and NK-YS [26], were treated with IL2 prior to analysis. IL2 stimulation resulted in the binding of NF-κB to its consensus sequences, as shown by the EMSA (Figure 1a), which demonstrated that IL2 activates NK tumour cells via the canonical NF-κB pathway involving the p65/p50 heterodimer. Consistently, more of the p65 subunit was detected in nuclear extracts from ENKL cells grown in the presence of IL2, while its cytosolic counterpart was unchanged (Figure 1b).

To address the role of Akt in this process, we treated the cells with an Akt-specific inhibitor (Akt-I) [27] before the addition of IL2. Akt-I is a phosphatidylinositol ether analogue that binds to the pleckstrin homology domain of Akt. We used a dosage of Akt-I that does not affect cell viability or PI3K (IC_{50} = 83 μM), such that other PI3K-related downstream signalling molecules remained unaffected. The addition of Akt-I inhibited the nuclear translocation of p65 and the binding of NF-κB to its consensus sequences (Figures 1a and 1b). To demonstrate the specific effect of this inhibitor on Akt activity, we examined the phosphorylation status of the Ser^{473} residue, a hallmark of Akt activation. As expected, Akt phosphorylation was increased in the cells treated with IL2 alone, whereas treatment of the cells with Akt-I for 4 h suppressed IL2-induced Akt phosphorylation (Figure 1c).

To evaluate NF-κB activity further under these conditions, semi-quantitative RT-PCR was performed to examine the RNA transcript levels of granzyme B and perforin. Granzyme B and perforin are the two major components of NK cell cytolytic granules and their genes are responsive to NF-κB [20,28]. The RT-PCR results showed that IL2 enhances the transcription

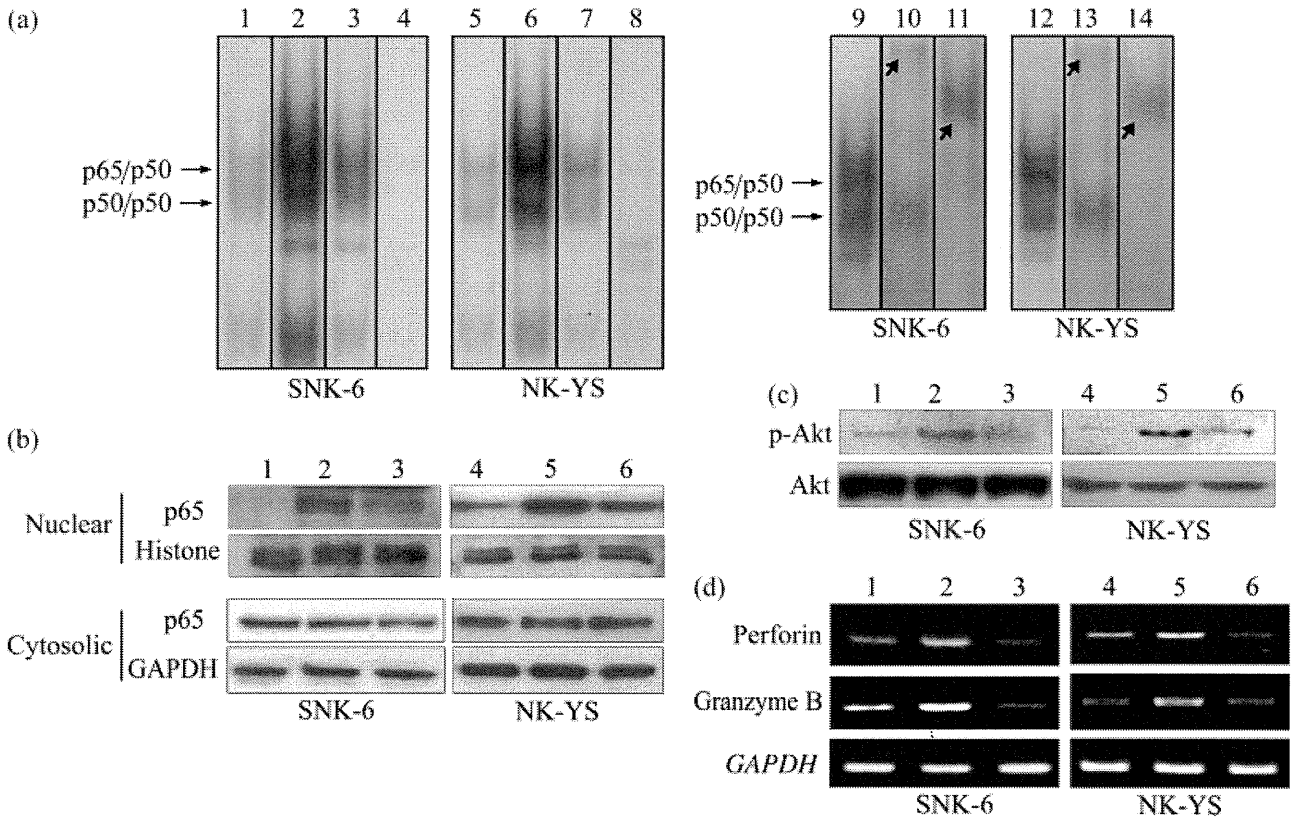

Figure 1. Activation of NF-κB via Akt. (a) EMSA results of NK cell lines SNK-6 and NK-YS. Cells were deprived of IL2 (1 and 5) or treated with 300 U/ml of IL2 alone (2, 6, 9, and 12) or IL2 together with 10 μM Akt-I (3 and 7). In the supershift assay, nuclear lysates were incubated with either p65 antibody (10 and 13) or p50 antibody (11 and 14) to identify the position (short-tailed arrows) of the p65/p50 heterodimer and the p50 homodimer. A cold competitor of the NF-κB consensus sequence was added as a control (4 and 8). (b) Immunoblotting results for p65 in nuclear and cytosolic extracts from the SNK-6 and NK-YS cell lines. GAPDH was used for the normalization of cytosolic proteins and histone H1 was used for the normalization of nuclear proteins. (c) Immunoblotting results for phospho-Akt (Ser^{473}), with total Akt used as the normalization control. (d) Semi-quantitative RT-PCR results for perforin and granzyme B. *GAPDH* was used for normalization. For b, c, and d, cells were deprived of IL2 (1 and 4) or treated with 300 U/ml IL2 alone (lanes 2 and 5) or IL2 together with 10 μM Akt-I (lanes 3 and 6).

of granzyme B and perforin, whereas Akt-I blocked this effect (Figure 1d).

IL2-induced NF-κB activation is BCL10-dependent

To explore the potential role of BCL10 in cytokine receptor signalling, the expression of BCL10 was knocked down using an shRNA specifically targeting BCL10. As demonstrated by western blot, sequence B suppressed BCL10 expression more effectively than sequence A (Figure 2a). Depletion of BCL10 rendered the SNK-6 cells less responsive to IL2 with regard to NF-κB activation, compared with treatment with the control sequence (Figure 2b). To rule out off-target silencing effects on Akt activation due to the shRNA, we again measured the levels of Akt phosphorylation in cells treated with shRNA. As shown in Figure 2c, no remarkable changes in Akt phosphorylation levels were observed between the mock control and the shRNA-treated cells. These results suggest that BCL10 participates in IL2-mediated NF-κB signalling and likely plays a role downstream of Akt.

We then examined the transcription of the cytolytic genes perforin and granzyme B, which is responsive to NF-κB. As expected, depletion of BCL10 resulted

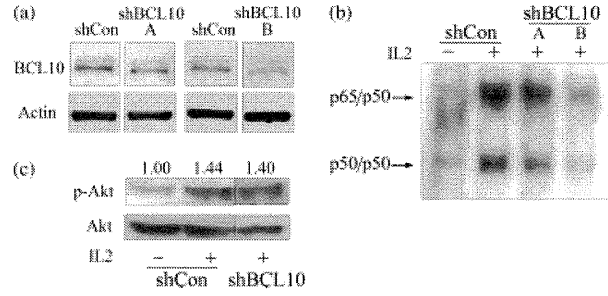

Figure 2. Knockdown of BCL10 expression inhibits IL2-induced NF-κB activation. (a) Immunoblotting results for BCL10 in SNK-6 cells. BCL10 expression was knocked down using two shRNA sequences (shBCL10-A and -B). A luciferase sequence (shCon) was used as a negative control. Actin served as the normalization control for immunoblotting. (b) EMSA results showing the changes in NF-κB activity in SNK-6 cells. (c) Immunoblotting results for phospho-Akt (p-Akt) in SNK-6 cells, with total Akt used as a normalization control. Band density was measured with Grab-IT (Ultra Violet Products Ltd, Cambridge, UK). The p-Akt to Akt ratio is shown at the top of the panel for comparison.

in a decline in the transcription of both perforin and granzyme B (Figure 3a). Furthermore, alterations in NF-κB activity were demonstrated by cell cycle analysis because the up-regulation of NF-κB activity

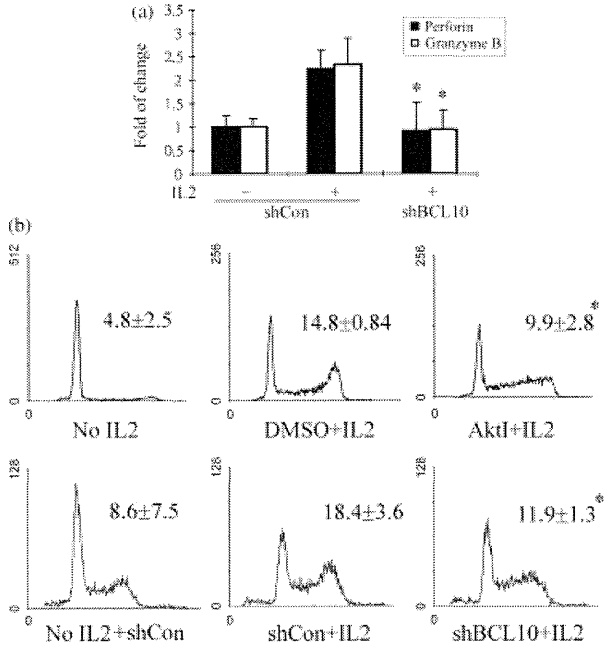

Figure 3. Knockdown of BCL10 suppresses IL2-induced gene transcription and restricts the number of cells in the G_2/M phase. (a) Quantitative RT-PCR results for perforin and granzyme B in SNK-6 cells. shRNA-transduced cells were treated in the presence or absence of IL2 as specified in the figure. (b) Blocking Akt or silencing BCL10 with shRNA reduced the percentage of SNK-6 cells in the G_2/M phase. DMSO was the vehicle control for Akt-I. A luciferase sequence (shCon) was used as a negative control for RNA interference in a and b. Each histogram is representative of three independent experiments. The percentage of cells in the G_2/M phase from three experiments is shown as the mean ± SD (*$p < 0.05$ when compared with the corresponding negative or vehicle control).

usually allows more cells to undergo cell division [29]. The addition of IL2 induced more SNK-6 cells to enter the cell cycle, with an increase in the percentage of cells in the G_2/M phase, but this effect could be suppressed by either Akt-I or shBCL10-B (Figure 3b).

IL2 promotes the overexpression and phosphorylation of BCL10

The *BCL10* gene has been suggested to be responsive to NF-κB [25]; we therefore examined the expression level of BCL10 in both cell lines treated with different concentrations of IL2. Incubation with IL2 for 4 h could either increase the total expression level or promote the phosphorylation of BCL10, but the results were slightly different between the two cell lines (Figure 4). In SNK-6 cells, there was an increase in the phosphorylated form of BCL10, but changes in the unphosphorylated form were not evident. In NK-YS cells, both forms seemed to be increased simultaneously along with IL2 in a dose-dependent manner.

IL2 induces BCL10 translocation to the nucleus

In addition to up-regulation of BCL10, IL2 stimulation could trigger the nuclear translocation of BCL10

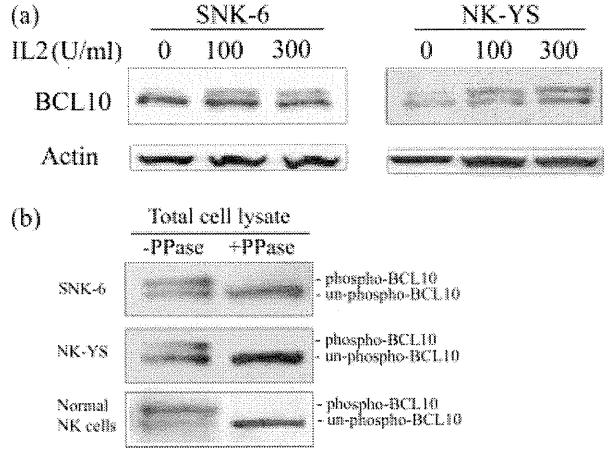

Figure 4. IL2 induces an increase in the total and phosphorylated forms of BCL10. (a) Immunoblotting results for BCL10 in NK cell lines treated with different concentrations of IL2. β-Actin served as the loading control. (b) Identification of phospho-BCL10 by phosphatase (λ-PPase) treatment and immunoblotting. Total cell lysates were incubated in the presence or absence of phosphatase for 4 h before western blotting.

in NK cells. The malignant cell lines (SNK-6 and NK-YS) and normal NK cells were cultured without the addition of IL2 for 2 days before they were stimulated with IL2. The addition of IL2 resulted in more BCL10 in the nucleus compared with the IL2-deprived cells. This phenomenon was observed not only in both ENKL cell lines, but also in IL2-activated NK cells from healthy individuals; thus, it was a result of the activation of NK cells rather than a lymphoma-specific effect. The BCL10 in the nucleus formed large granules with irregular shapes (Figure 5a). Moreover, the western blot results were consistent with the finding that BCL10 levels increased significantly in nuclear extracts upon IL2 stimulation (Figure 5b), while they increased only slightly in the cytosolic extracts. Like its cytosolic counterpart, nuclear BCL10 was also made up of both phosphorylated and unphosphorylated forms, suggesting that BCL10 phosphorylation alone is not sufficient for nuclear translocation. The nuclear translocation was Akt-dependent, however, as the addition of Akt-I reduced the amount of nuclear BCL10 but did not change that of cytosolic BCL10 (Figure 5c).

BCL3 is a binding partner of BCL10

The translocation of BCL10 has been shown to be aided by another molecule, BCL3, in the human breast carcinoma cell line MCF7 [25] and the diffuse large B-cell lymphoma cell line Pfeiffer [30]. A small-scale yeast two-hybrid screen identified BCL3 as a potential binding partner of BCL10 in our NK tumour cell lines (data not shown). To further confirm the potential interaction between these two molecules, we enriched BCL10 from the crude protein lysates by immunoprecipitation and examined whether BCL3 is a binding partner of BCL10 by western blotting. As shown in Figure 6, the BCL10 antibody was able to

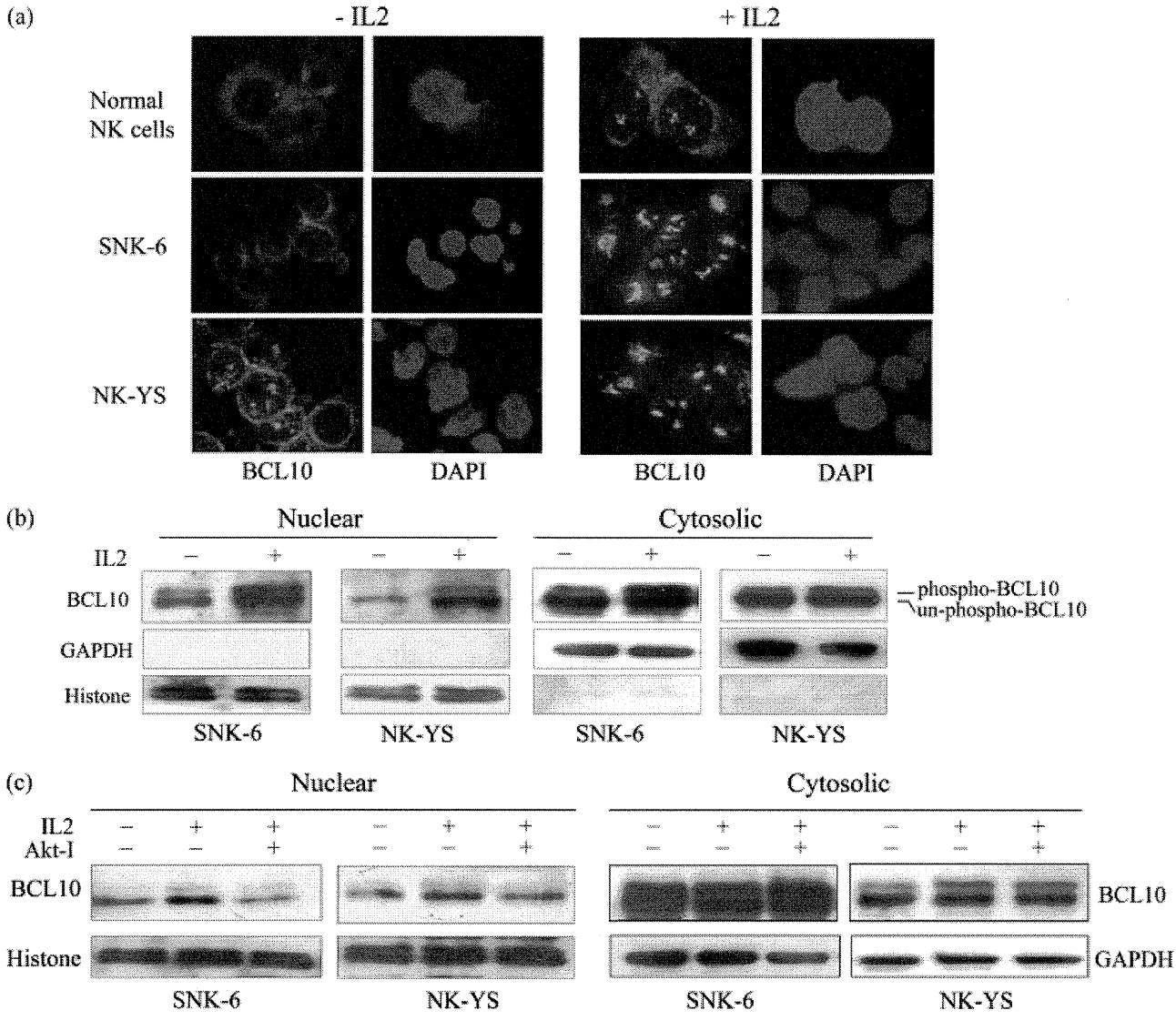

Figure 5. IL2 induces the nuclear translocation of BCL10 in normal and neoplastic NK cells. (a) Immunofluorescence micrographs of the NK-cell cytospin preparations. NK cells were cultured for 24 h in the presence or absence of IL2 (original magnification 400×). BCL10 was detected with a FITC-conjugated antibody (green) and the nuclei were stained with DAPI (blue). (b) Immunoblotting results for BCL10 in protein extracts from subcellular fractionation. GAPDH and histone served as the normalization controls for cytosolic and nuclear proteins, respectively. (c) Immunoblotting results for BCL10 in nuclear and cytosolic extracts from the NK cell lines. The combination of IL2 (300 U/ml) and Akt-I (10 μM) is specified in the figure. GAPDH and histone were used as loading controls for the cytosolic and nuclear extracts, respectively.

co-immunoprecipitate BCL3 in both SNK-6 and NK-YS cells, indicating that they form a complex in these IL2-activated NK cells.

IL2 induces BCL3 overexpression and translocation to the nucleus

We next investigated the molecular response of BCL3 following IL2 stimulation by examining the expression of BCL3 at both the transcriptional and the translational levels. IL2 induced increases in the mRNA and protein levels of BCL3 (Figures 7a and 7b). This effect was again blocked by Akt-I, showing the involvement of the PI3K/Akt pathway (Figure 7c). We next examined whether IL2 could induce the nuclear translocation of BCL3. Western blot analysis showed that more BCL3 was present in both the nuclear and the cytosolic fractions of NK cell lines when they were grown in the presence of IL2 (Figure 7d). Treatment with Akt-I reduced the amount of nuclear and cytosolic BCL3, suggesting that BCL3 expression was affected. Thus, the decrease in the level of nuclear BCL3 must be a result of the down-regulation of BCL3 expression caused by Akt-I.

BCL3 plays a role in the subcellular localization of BCL10

To clarify further the role of BCL3 in the nuclear transfer of BCL10, we used shRNA to suppress the expression of BCL3 and evaluated the subsequent effects on BCL10 subcellular localization. Two sequences targeting *BCL3* mRNA were examined and sequence B was selected to knock down BCL3 expression in

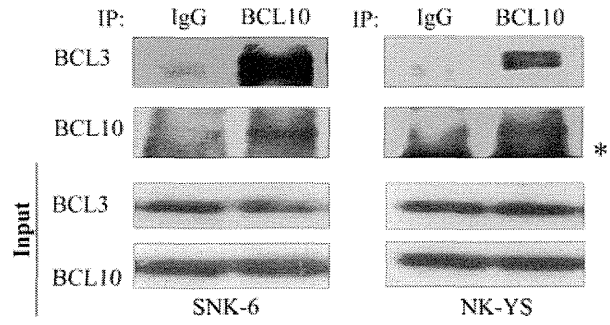

Figure 6. Co-immunoprecipitation of BCL3 with BCL10. An interaction between BCL3 and BCL10 was demonstrated by immunoprecipitation. Whole cell extracts were immunoprecipitated with an anti-BCL10 antibody or isotype-matched IgG (control). The purified product was examined with antibodies against BCL3 and BCL10 by immunoblotting. The asterisk indicates non-specific bands from the immunoglobulin light chains. The 'Input' control shows that the same amount of protein was used for immunoprecipitation.

subsequent experiments (Figure 8a). After infection with the retrovirus carrying the shRNA sequence, SNK-6 cells showed a decrease in BCL3 expression in both the nuclear and the cytosolic extracts. Notably, BCL10 expression decreased along with BCL3 in the nuclear fractions, while cytosolic BCL10 expression remained unchanged (Figure 8b). To identify whether *de novo* protein synthesis is necessary for the translocation, we treated the cells with cycloheximide (CHX), a protein synthesis inhibitor, before stimulation with IL2. This treatment blocked the presence of BCL10 and BCL3 in the nuclear fractions and BCL3 in the cytosolic fractions (Figure 8c). There was a considerable amount of BCL10 in the cytosolic fractions, however, as it is more stable than BCL3. This result suggests that *de novo* synthesis of both BCL10 and BCL3 is necessary for their appearance in the nucleus in response to IL2.

Discussion

Cytokine receptor-induced lymphocyte activation often plays a role in the inflammatory and immune responses that occasionally give rise to lymphomagenesis [31,32]. In low-grade MALT lymphoma, the growth of tumour cells is maintained by stimulating signals from pro-inflammatory cytokines produced during chronic gastritis with persistent infection by *Helicobacter pylori*. Antibiotics that kill *H. pylori* block lymphocyte activation signalling, curing the gastritis and even the MALT lymphoma itself [33,34]. Similarly, ENKL is a lymphoid malignancy associated with Epstein–Barr virus infection [35]. A latent viral product such as LMP1 can up-regulate the expression of different cytokines, including interferon and IL10 [36,37]. Moreover, NK lymphoma cells are functionally active in a cytolytic manner and are characterized by constitutive activation of NF-κB [2], suggesting that cytokine-driven lymphocyte activation is essential for the development of NK cell lymphoma.

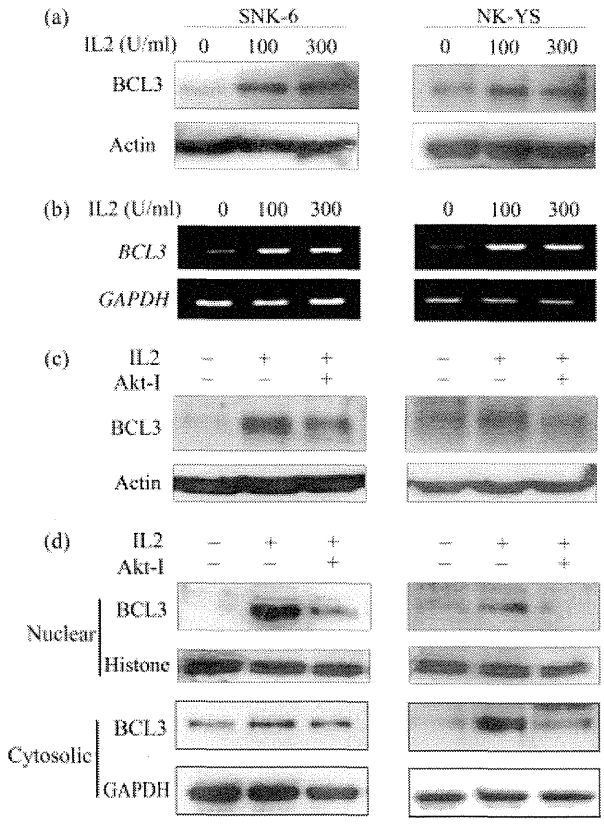

Figure 7. IL2 increases the transcript and protein levels of BCL3. Immunoblotting (a) and RT-PCR results (b) for BCL3 expression in NK cell lines treated with different concentrations of IL2. Actin and GAPDH were used as the normalization controls for a and b, respectively. (c) Immunoblotting results for BCL3 expression. Actin served as the normalization control. (d) Change in the amount of BCL3 in the nuclear and cytosolic extracts. GAPDH and histone were used as loading controls for the cytosolic and nuclear extracts, respectively. For c and d, the combination of IL2 (300 U/ml) or Akt-I (10 μM) is specified in the figure.

With regard to the use of IL2 as a model to study cytokine-driven NF-κB activation, we believe that IL2 is likely among the few cytokines that promote tumourigenesis in NK cell malignancies. It is required to maintain NK cell proliferation *in vitro*, and primary NK cells in human lymph nodes are dependent on T-cell-derived IL2 for cytotoxicity, in addition to viability and proliferation [19]. ENKLs are neoplasms with a cytotoxic NK phenotype [2]. ENKL cells do not express IL2 [38], but reactive T cells in the tumour micro-environment are likely a major source of IL2. Tumour-infiltrating T cells are prevalent in ENKL specimens [39–41] and frequently, they are the major cell population within the primary site and metastases of ENKL [41]. Conceivably IL-2 can be provided by activated T cells *in vivo* in ENKLs.

In the present study, we demonstrated that IL2 triggers NF-κB activation through the Akt pathway. Extensive studies have shown that BCL10 is a key mediator of NF-κB signalling in lymphocytes [42,43]. Along with its conventional role in antigen receptor signalling, recent studies have shown the involvement of BCL10 in mediating NF-κB signalling downstream of G protein-coupled receptors and Toll-like receptors

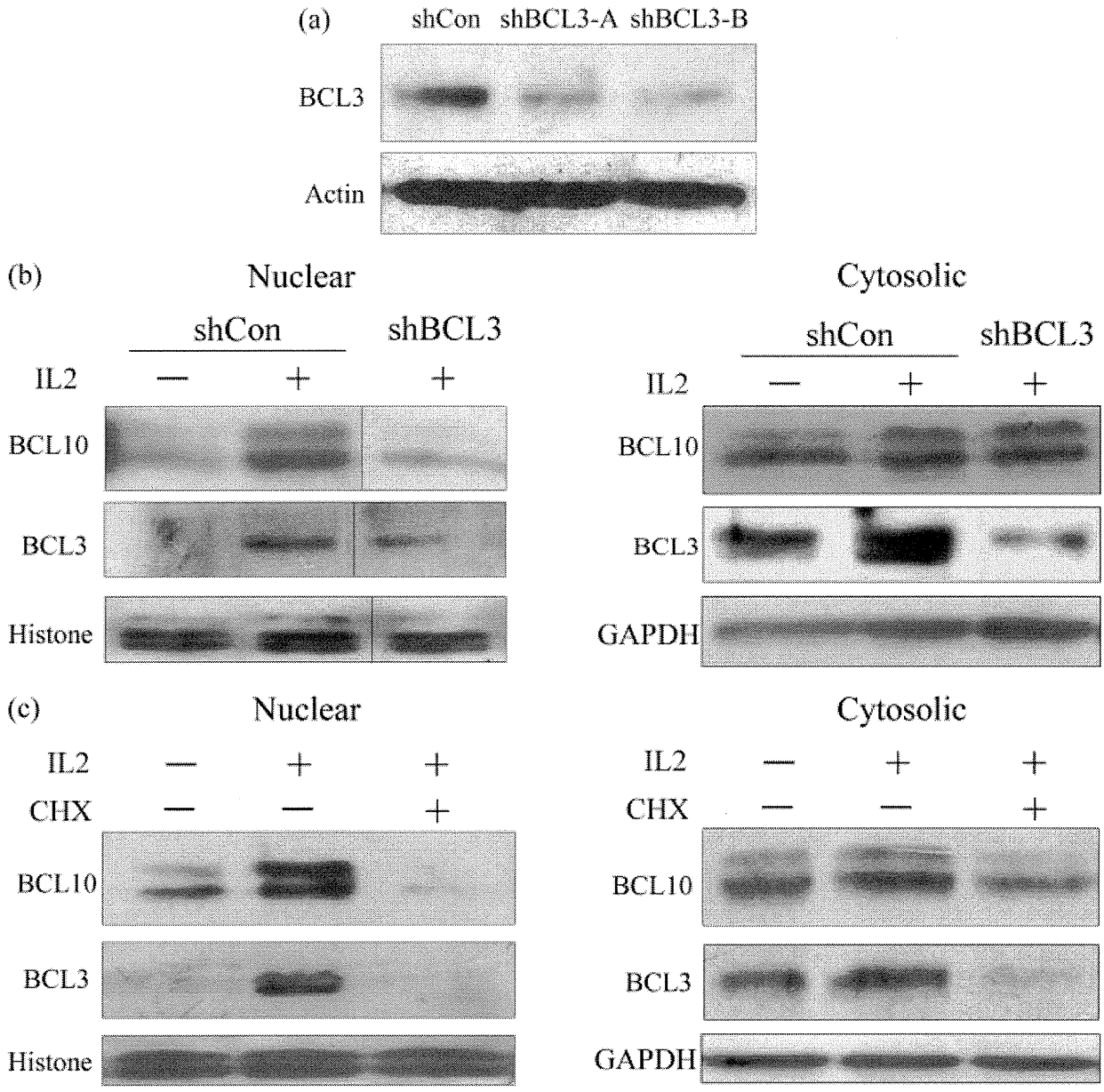

Figure 8. Knockdown of BCL3 expression by shRNA or CHX affects the nuclear localization of BCL10. (a) Immunoblotting results for BCL3 in SNK-6 cells. The expression of BCL3 was knocked down using two shRNA sequences. Actin served as the normalization control for immunoblotting. (b) Immunoblotting result for BCL10 and BCL3 in the nuclear and cytosolic extracts. shRNA-transduced SNK-6 cells were grown in the presence or absence of IL2 (300 U/ml) before cellular fractionation. (c) Immunoblotting results for BCL10 and BCL3 in the nuclear and cytosolic extracts. NK-YS cells were treated with IL2 in the presence or absence of 80 μg/ml CHX for 24 h before cellular fractionation. For b and c, GAPDH and histone were used as loading controls for the cytosolic and nuclear extracts, respectively.

[44,45]. Here we have provided evidence that BCL10 also participates in cytokine receptor-induced NF-κB signalling. Similar to the role of PKC in antigen receptor signalling, Akt is the kinase responsible for signal transduction via the IL2 receptor. Downstream of these kinases, BCL10 acts as a conductor to orchestrate NF-κB activation signalling, which is linked to different receptors, suggesting that BCL10 is a crucial adaptor in immune cells.

The nuclear localization of BCL10 is a recurrent phenomenon associated with MALT lymphoma and ENKL [4,46], indicating that aberrant nuclear BCL10 expression might play a role in the development of these diseases. Moreover, a distinct group of MALT lymphoma patients have shorter failure-free survival associated with the presence of nuclear BCL10 [47]. Thus, the identification of mechanisms that regulate the subcellular localization of BCL10 may be beneficial. An earlier report indicated that BCL3, a member of the IκB family, may be a binding partner of BCL10 in the nucleus [25]. That study focused on the human breast carcinoma cell line MCF7, however, raising concerns that the findings may not be representative of the actions of BCL3 in lymphoid cells. Kuo *et al* recently reported that B-cell activating factor (BAFF), a tumour necrosis factor-related cytokine, induces the nuclear transfer of BCL10 via BCL3 in the B-cell lymphoma cell line Pfeiffer [30]. Here we have described a similar

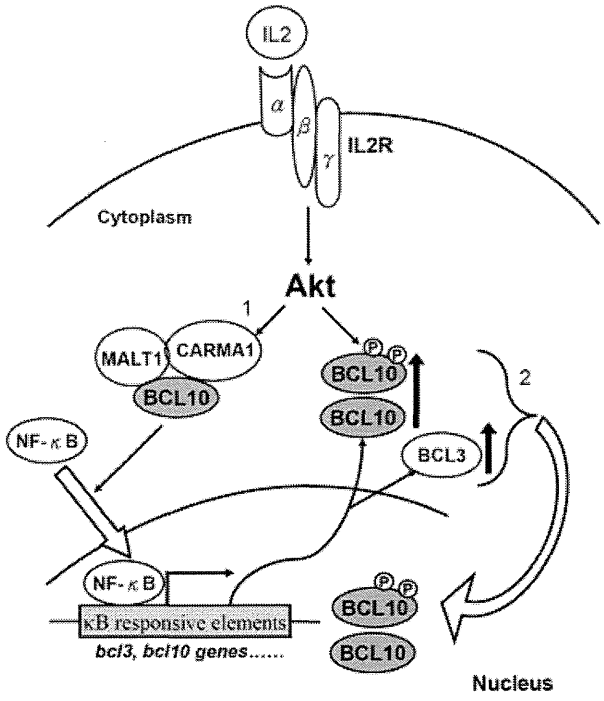

Figure 9. Schematic diagram of BCL3/BCL10-mediated NF-κB signalling modulation in ENKL. (1) Engagement of the IL2 receptor with IL2 activates the canonical NF-κB signalling pathway via Akt and this leads to a global increase in the expression of NF-κB-responsive genes. BCL3 and BCL10 expression are up-regulated and more protein appears in the cytosol. A circuit of BCL10 overexpression forms and promotes NF-κB activation. (2) On the other hand, BCL3 binds to BCL10 and facilitates BCL10 nuclear translocation. The level of BCL10 decreases in the cytosol and formation of the CARMA1–BCL10–MALT1 signalosome is inhibited. This negative feedback modulates NF-κB signalling.

scenario, demonstrating that IL2 induces the nuclear localization of both BCL3 and BCL10 in ENKL cells. This study provides an underlying mechanism for the nuclear translocation of BCL10 and more significantly, we have identified the essential role of BCL10 that connects IL2 receptor signalling with NF-κB activation. Because IL2 is a cytokine that plays a crucial role in the proliferation and development of T, B, and NK cells [48], the identification of BCL10 in the NK-cell activation signalling pathway that links the IL2 receptor with NF-κB activation is of great significance.

In Figure 8 we show that BCL10 nuclear translocation is dependent on the availability of BCL3. When BCL3 was silenced by RNA interference, BCL10 nuclear translocation was suppressed accordingly. Furthermore, when overall protein translation was suppressed by CHX, the nuclear transfer of BCL10 was diminished. This indicates that the nuclear translocation of BCL3 and BCL10 is dependent on the availability of new proteins, which are continuously generated. Overexpression of BCL3 may promote the nuclear translocation of BCL10. On the other hand, BCL3 is a member of the IκB family that does not act on the IKK complex. It plays a role as an NF-κB co-activator in the nucleus and is believed to be oncogenic [49]. Overexpression of BCL3 has been detected in multiple types of leukaemias and lymphomas [50]. Besides its role as a BCL10 binding partner, BCL3 has other roles that may also contribute to tumourigenesis.

As shown in Figure 9, up-regulation of BCL10 expression may occur via NF-κB binding to its potential 5′ UTR [25], which will transduce more activating signals through the amplification loop from BCL10 to NF-κB. The excess amount of BCL10 may exceed the number of MALT1 molecules, allowing BCL10 to escape cytosolic retention by MALT1 and enter into the nucleus [8,51]. Up-regulation of BCL3 would allow it to carry more BCL10 into the nucleus. If more BCL10 translocates into nucleus, the excess of BCL10 in the cytosol—where the CARMA1–BCL10–MALT1 signalosome is formed and plays a role in NF-κB signalling—would be reduced. Therefore, nuclear translocation of BCL10 is a result of NF-κB activation and in turn, it is used to modulate NF-κB signalling. A recent report also suggested that BCL10 in the nucleus is subject to degradation via the proteasome [52]. Thus, the nuclear translocation of BCL10 could represent a feedback mechanism that modulates 'exaggerated' NF-κB signalling. Other functions of nuclear BCL10, however, remain to be determined.

In summary, we have identified a critical role for BCL10 in cytokine receptor-induced NF-κB signalling, which results in NK cell activation. We also determined the underlying mechanism of the nuclear translocation of BCL10, which was found to be associated with constitutive NF-κB activation. Given that knockdown of BCL10 by shBCL10 suppressed the IL2-induced entry of SNK-6 cells into the G2/M phase of the cell cycle (an anti-proliferative effect), silencing of BCL10 might be a potential therapeutic option to kill ENKL tumour cells.

Acknowledgment

This study was supported by the General Research Fund (GRF) of the Research Grants Council of Hong Kong, China (HKU 7583/54M to GS and RHS).

References

1. Jaffe E, Chan J, Su I, Frizzera G, Mori S, Feller AC, *et al.* Report of the workshop on nasal and related extranodal angiocentric T/natural killer cell lymphomas. Definitions, differential diagnosis, and epidemiology. *Am J Surg Pathol* 1996; **20**: 103–111.
2. Chiang A, Chan A, Srivastava G, Ho F. Nasal NK/T-cell lymphomas are derived from Epstein–Barr virus-infected cytotoxic lymphocytes of both NK- and T-cell lineage. *Int J Cancer* 1997; **73**: 332–338.
3. Kaneko T, Fukuda J, Yoshihara T, Zheng H, Mori S, Mizoguchi H, *et al.* Nasal natural killer (NK) cell lymphoma: report of a case with activated NK cells containing Epstein–Barr virus and expressing CD21 antigen, and comparative studies of their phenotype and cytotoxicity with normal NK cells. *Br J Haematol* 1995; **91**: 355–361.
4. Shen L, Liang ACT, Lu L, Au WY, Wong KY, Tin PC, *et al.* Aberrant BCL10 nuclear expression in nasal NK/T-cell lymphoma. *Blood* 2003; **102**: 1553–1554.